

Ru Shien TAN, Tuan Amran TUAN ABDULLAH, Anwar JOHARI, Khairuddin MD ISA

Catalytic steam reforming of tar for enhancing hydrogen production from biomass gasification: a review

© Higher Education Press 2020

Abstract Presently, the global search for alternative renewable energy sources is rising due to the depletion of fossil fuel and rising greenhouse gas (GHG) emissions. Among alternatives, hydrogen (H_2) produced from biomass gasification is considered a green energy sector, due to its environmentally friendly, sustainable, and renewable characteristics. However, tar formation along with syngas is a severe impediment to biomass conversion efficiency, which results in process-related problems. Typically, tar consists of various hydrocarbons (HCs), which are also sources for syngas. Hence, catalytic steam reforming is an effective technique to address tar formation and improve H_2 production from biomass gasification. Of the various classes in existence, supported metal catalysts are considered the most promising. This paper focuses on the current researching status, prospects, and challenges of steam reforming of gasified biomass tar. Besides, it includes recent developments in tar compositional analysis, supported metal catalysts, along with the reactions and process conditions for catalytic steam reforming. Moreover, it discusses alternatives such as dry and autothermal reforming of tar.

Keywords hydrogen, biomass gasification, tar, steam reforming, catalyst

1 Introduction

The rapid depletion of fossil fuels and associated

Received May 12, 2019; accepted Sept. 26, 2019; online Mar. 30, 2020

Ru Shien TAN, Tuan Amran TUAN ABDULLAH (✉),
Anwar JOHARI
Centre of Hydrogen Energy, Institute of Future Energy; School of
Chemical and Energy Engineering, Faculty of Engineering, Universiti
Teknologi Malaysia, 81310 Skudai, Johor, Malaysia
E-mail: tuanamran@utm.my

Khairuddin MD ISA
School of Environmental Engineering, Universiti Malaysia Perlis,
Kompleks Pusat Pengajian Jejawi 3, 02600 Arau, Perlis, Malaysia

environmental issues such as global warming and climate change are becoming global concerns [1]. Carbon dioxide (CO_2) is deemed as the principal greenhouse gas (GHG) [2,3]. It constitutes approximately 82% of GHG that contribute to global warming [4]. Based on the report from the United States Environmental Protection Agency, fossil fuel combustion is the largest source of emissions accounting for 80.9% of the total CO_2 emissions in 2014 [5]. It is estimated that the increase in global temperatures by $1.9^\circ C$ and sea level expansions of 3.8 m [6,7] may result in the extinction of 15 to 40 threatened species worldwide [8]. However, the global energy demand is continuously increasing at an alarming rate year after year [9]. In 2017, fossil fuels accounted for 81% of the global electricity generation compared to other sources of energy [10]. Therefore, the global search for alternative renewable energy sources as a replacement for conventional fossil fuels has become a necessity.

Among the alternatives, hydrogen (H_2) is considered a practical approach to generate electricity in the 21st century sustainably. In addition, H_2 has the highest energy density (122 MJ/kg) among existing fuels. Its energy yield is approximately 2.75 times higher than that of most hydrocarbons (HCs) [11]. However, H_2 does not occur naturally on the earth but commonly exists as part of other substances in nature such as water, alcohol, natural gas, biomass, coal, and hydrocarbon [12]. Consequently, it can only be obtained from H_2 -containing resources through chemical reaction processes. The diversity of sources makes H_2 a promising energy carrier for the future [12,13]. By employing H_2 gas, the crises of supply disruption and the impact of GHG emissions associated with conventional fossil fuel-based energy systems can be avoided, as depicted as Fig. 1. The reason for this is that H_2 utilization generates only water vapor as a by-product with zero GHG emissions during fuel cell application [14,15]. For these reasons, great efforts should be committed to exploiting the production of H_2 .

In recent years, numerous technologies including thermochemical conversion [11,16–18], electrolysis

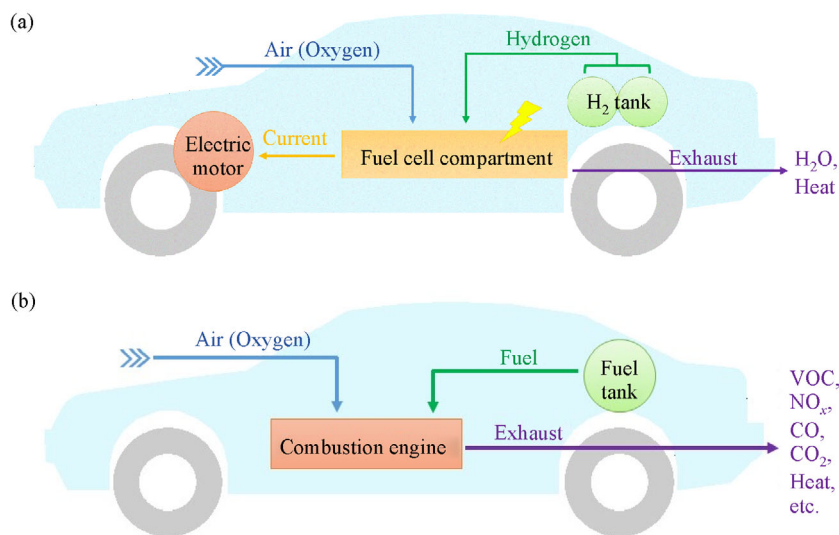


Fig. 1 Comparison between (a) fuel cell vehicle and (b) conventional vehicle.

[19,20], and photolysis [21,22] are under development for H₂ production. Natural gas steam reforming has been used in the industry over the years. The polymer membrane electrolyte (PEM) electrolyzer technology has also been developed for commercial applications. However, electrolysis consumes the most energy among these technologies [23]. Besides, the low efficiency of photolysis-based H₂ production rate currently makes it a commercially unfeasible technology. Among these possible options, H₂ production from biomass gasification is considered an economical and promising technology due to its carbon neutrality, environmentally friendly, sustainable, and renewable characteristics [24–26]. Therefore, biomass thermochemical conversion can be practised in the near term and is deemed as a potential technology in the long-term [27]. However, significant tar formation along with raw syngas is a serious impediment to the development and deployment of biomass gasification [28]. Hence, it is necessary to solve the tar problem of gasification to make the method more attractive for commercialization.

Typically, the tar content in syngas produced from biomass gasification ranges from 0.5 to 100 g/Nm³ [29,30]. However, the tolerance limit of tar in syngas for various applications is 1, 5, and 100 mg/Nm³ in fuel cells, gas turbines, and internal combustion engines, respectively [30]. Tar condenses at low temperatures, subsequently resulting in syngas end-used or process-related problems which typically include blockages and corrosion in downstream filters, fuel lines, engine nozzles, and turbines [31,32] as well as bad odour issues around the gasification plant. Furthermore, the formation of tar represents a decrease in conversion efficiency since biomass is converted to tar instead of syngas.

To date, several strategies aimed at raw syngas purification, including physical separation such as wet

scrubbing [33], filtration [34], and electrostatic precipitation [35] have been attempted. Although physical separation considerably removes tar from raw syngas, it has great potential to create secondary pollution. Since tar is a complex mixture of HCs, it is more practical to convert tar into valuable H₂ gas through thermochemical processes such as catalytic reforming, thermal, and catalytic cracking [36]. Hence, the physical removal and further reduction/oxidation of tar are essential to improve the H₂ production with minimal wastes.

Steam reforming is a promising technique that provides a conversion mechanism for liquid HCs [12]. It offers a higher concentration of H₂ in the reformat which is about 70% to 80% (vol.) on a dry basis compared to other reforming technologies (40%–50% (vol.)) [37]. In addition, it produces about 100000 Nm³/h of H₂ gas on an industrial scale [38]. The resulting cost of H₂ by steam reforming is \$3.38/kg H₂ or the equivalent of \$1.55/gal for gasoline [39]. Besides, dry reforming and autothermal reforming of tar are also currently investigated by some researchers but the study of these technologies is still in an early stage.

A catalyst is any chemical substance that lowers the activation energy to accelerate the chemical reaction rate of steam reforming without being consumed in the process [40]. In recent years, several supported metal catalysts have been developed and utilized for laboratory-scale steam reforming of tar. Typically, the non-noble transition metals (Ni [41], Fe [42], and Co [43]) and noble metals (Pt [44], Ru [45], and Pd [46]) are adopted as the active metal in steam reforming catalysts. Besides, metal oxide [24], rare earth oxide [47], olivine [42], calcined rocks [48], and clay minerals [49] are adopted as support in steam reforming catalysts.

So far, numerous supported catalysts have been

extensively developed and investigated for tar steam reforming. However, a relevant review in this field is currently lacking in the literature. Therefore, it is worthwhile to critically review the current research, challenges, and prospects of supported catalysts for the steam reforming of tar generated from biomass gasification reported over the past five years. The objective of the present paper is also to provide a state-of-the-art overview of catalytic reforming studies of gasified biomass tar for H_2 production.

2 Gasified biomass tar

Biomass is a sustainable and renewable organic source that consists of agricultural, forestry, municipal solid, and animal waste residues [50]. The utilization of biomass as feedstock for gasification is environmentally benign compared to non-renewable resources. Therefore, biomass gasification has become a popular technology for H_2

production [51]. However, the formation of tar along with syngas is a major drawback of biomass gasification [28].

Figure 2 presents the biomass gasification route and the proposed technique for improving syngas production by steam reforming of tar discharged from the gasifier. The biomass gasification process is controlled in an atmosphere with the presence of a gasifying agent (air, steam or a combination of these) and high temperatures ranging from 600°C to 1000°C [52]. Tar is separated from the raw syngas using a wet scrubber, which subsequently undergoes a steam reforming reaction to produce more syngas. Next, the syngas is purified by the CO shift reactor and pressure swing adsorption to obtain pure H_2 gas as a fuel for electricity generation and H_2 vehicle application. However, a portion of the syngas is sent to the industry for chemical and liquid fuel manufacturing.

Tar consists of various condensable HCs ranging from monocyclic to polycyclic aromatic HCs along with primary oxygenated to tertiary deoxygenated HCs [53]. Moreover, nitrogen-polycyclic aromatic HCs are also

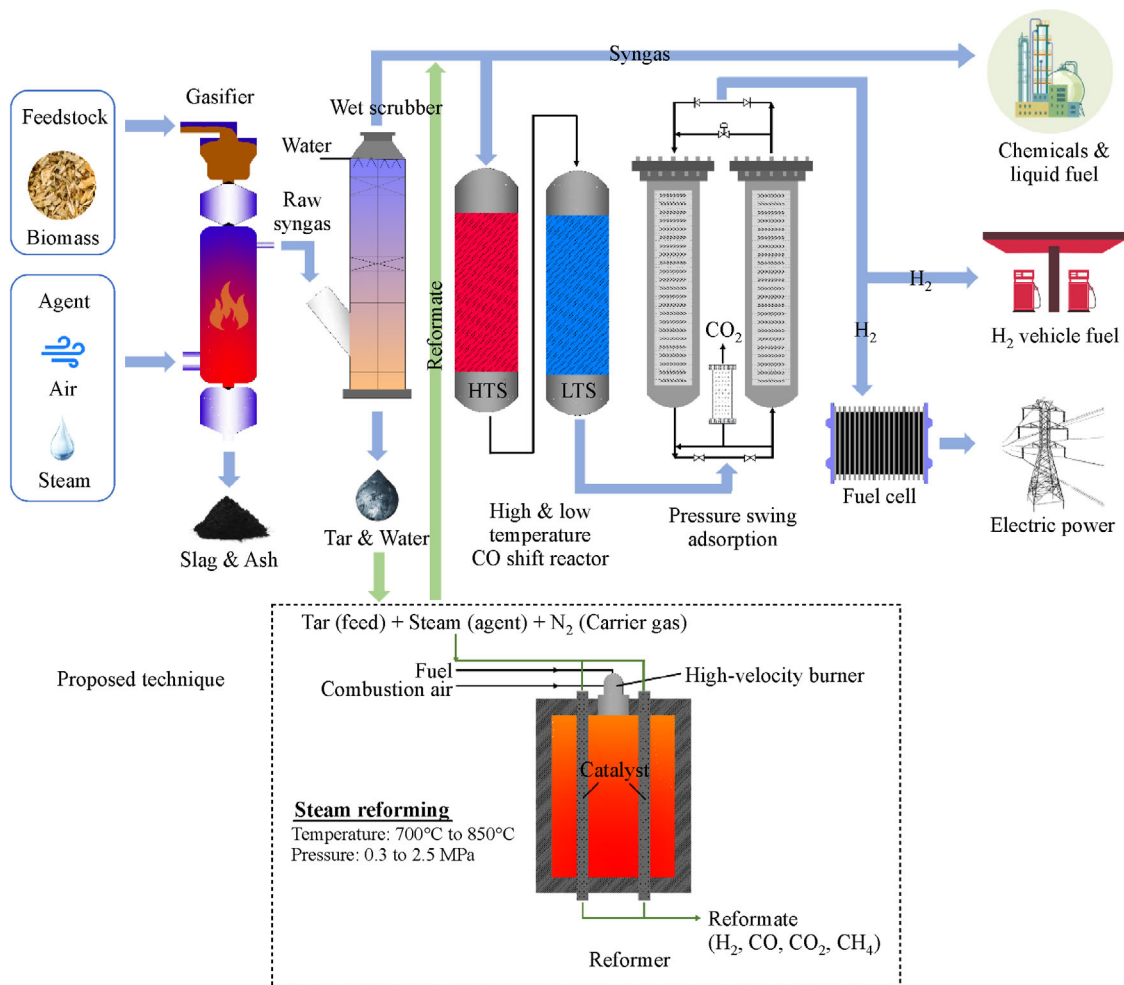


Fig. 2 A possible route of biomass gasification and proposed technique for improvement of syngas production.

generated during biomass gasification such as isoquinoline, pyridine, and quinoline [53,54]. The formation of tar is dependent on several gasification parameters including the selected feedstock [55], gasifier [56,57], reaction time [58,59], temperature [58,59], and gasifying agent [60].

Yu et al. [55] examined the formation of tar during biomass gasification. The findings show that lignin exhibits a higher yield, which causes the formation of more complex tar components compared to cellulose and hemicellulose. Furthermore, an updraft gasifier produces a larger quantity of tar (12000 mg/Nm^3) compared to a downdraft gasifier ($100\text{--}150 \text{ mg/Nm}^3$) [56,57]. According to Berruoco et al. [58] and Erkiaga et al. [59], the total tar yield decreases with the increase in reaction temperature and time. In terms of gasifying agent, tar formation can be significantly reduced by introducing steam and O_2 during gasification [60]. The reason for this is that O_2 accelerates the destruction of primary tar and conversion of phenolic to aromatic compounds [61]. Furthermore, the presence of steam prevents the polymerization reaction during gasification [60].

Figure 3 illustrates the composition of tar derived from gasification of various biomass feedstocks in the literature [62–65]. To facilitate sampling and analysis, tar can be categorized into five (5) classes according to its molecular weight (see Table 1). Due to the condensation characteristics of classes 1, 4, and 5 tars, fouling and clogging remains a problem in the downstream process. However, classes 2 and 3, tars are typically responsible for catalytic deactivation through compete on for active sites on the catalysts [53].

3 Steam reforming of gasified biomass tar

Among the reforming methods, steam reforming has the highest efficiency. Hence, it is a deep-rooted conversion

technology that produces H_2 rich gas using HCs as feedstock at high temperatures from 700°C to 900°C and pressures from 0.3 to 2.5 MPa in the presence of metal-based catalyst [66]. The main target of steam reforming is to obtain a high H_2 yield with the minimum CO content [67,68]. For example, using toluene as a feedstock, the H_2/CO ratio produced by steam, dry, and autothermal reforming is 1.57, 0.29, and 0.71, respectively. Therefore, steam reforming is the most preferred process for integration into tar removal techniques and conversion tar into valuable H_2 rich gas.

During steam reforming, numerous parallel reactions (see Table 2 and Fig. 4) occur simultaneously. As a result, the competing processes result in the formation and distribution of different products, namely, H_2 , CO, CO_2 , and CH_4 . The two main reversible reactions involved in steam reforming are the strongly endothermic reforming reactions (Eq. (1) for HCs and Eq. (2) for oxygenated HCs) [24,69], followed by a moderately exothermic water-gas shift reaction (Eq. (3)). In addition, the steam reforming of tar is typically accompanied by coke formation (Eq. (7)) on the catalyst surface, which can result in deactivation [70,71]. However, the catalyst deactivation can be prevented by carefully controlling the ratio of H_2O and CO_2 through Eqs. (8) and (9) where C is the deposited carbonaceous species [70–72].

4 Catalysts development of gasified biomass tar steam reforming

The current research on supported catalysts designed for the steam reforming of gasified biomass tar declared over the past five years is reviewed and discussed in this section. The catalyst types discussed in this section include Ni-based, other metal based-, promoted, alloy, supported, perovskite and hydrotalcite catalysts. The steam reforming

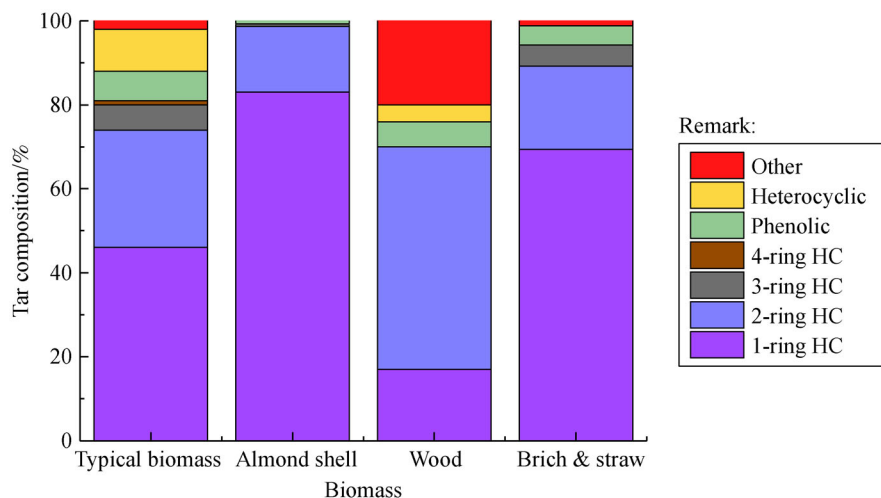


Fig. 3 Composition of gasified biomass tar derived from various biomass feedstock.

Table 1 Tar classification based on molecular weight [53]

Class	Description	Properties	Example
1	GC-undetectable	Heaviest tars, condensable at high temperature	–
2	Heterocyclic aromatic HC	Highly water-soluble	Pyridine, phenol, cresols, quinoline, isoquinoline and dibenzophenol
3	Light aromatic HC (1 ring)	Do not pose a condensation and solubility related problem	Toluene, ethylbenzene, xylenes, styrene
4	Light polycyclic aromatic HC (2–3 rings)	Condensable at low temperature even with low concentration	Indene, naphthalene, fluorine, phenanthrene and anthracene
5	Heavy polycyclic aromatic HC (4–7 rings)	Condensable at high temperatures even with low concentration	Fluoranthene, pyrene, chrysene, perylene and coronene

Table 2 Possible reactions involved in gasified biomass tar steam reforming process

Reaction	$\Delta H_{298}^0 / (\text{kJ} \cdot \text{mol}^{-1})$	Refs.
Steam reforming of hydrocarbon	> 0	[24,69]
$\text{C}_x\text{H}_y + x\text{H}_2\text{O} \rightleftharpoons \left(x + \frac{1}{2}y\right)\text{H}_2 + \text{CO} \quad (1)$	> 0	[24,69]
Steam reforming of oxygenated hydrocarbon		
$\text{C}_x\text{H}_y\text{O}_z + (x-z)\text{H}_2\text{O} \rightleftharpoons \left(x + \frac{1}{2}y - z\right)\text{H}_2 + x\text{CO} \quad (2)$		
Water-gas shift	–41	[72,73]
$\text{CO} + \text{H}_2\text{O} \rightleftharpoons \text{CO}_2 + \text{H}_2 \quad (3)$		
Dry reforming	> 0	[48,74]
$\text{C}_x\text{O}_y + x\text{CO}_2 \rightleftharpoons \frac{1}{2}y\text{H}_2 + 2x\text{CO} \quad (4)$		
Hydrodealkylation	< 0	[74,75]
$\text{C}_x\text{H}_y + \text{H}_2 \rightarrow \text{C}_{x-1}\text{H}_{y-2} + \text{CH}_4 \quad (5)$		
Methane steam reforming	206.9	[74,75]
$\text{CH}_4 + \text{H}_2\text{O} (\text{g}) \rightleftharpoons \text{CO} + 3\text{H}_2 \quad (6)$		
Carbon formation	< 0	[70,71]
$\text{C}_x\text{H}_y \rightarrow x\text{C} + \frac{1}{2}y\text{H}_2 \quad (7)$		
Boudouard reaction	172	[70,72]
$\text{C} + \text{CO}_2 \rightleftharpoons 2\text{CO} \quad (8)$		
Carbon gasification	131	[70,71]
$\text{C} + \text{H}_2\text{O} \rightleftharpoons \text{CO} + \text{H}_2 \quad (9)$		

processes of gasified biomass tar are summarized in Table 3.

4.1 Ni-based catalysts

From an industrial standpoint, the application of Ni-based catalyst is more practical because of its economic feasibility and marked performance in C-H, C-C, and O-H bonds cleavage [24,76]. However, it is prone to deactivation by sintering [77,78] and coke formation [78–80] on active sites. The performance of Ni/red cedar

activated char derived from various precursors in steam reforming of toluene and naphthalene/toluene mixtures was evaluated by Qian and Kumar [41]. It was found that nickel nitrate derived catalyst was more active in toluene conversion than those derived from nickel acetate. In this case, both Ni precursors showed a similar textural property of the catalyst in terms of specific surface area, pore volume, and pore size. This indicates that the better performance of nickel nitrate derived catalyst is mainly attributed to its smaller metallic size and higher Ni dispersion.

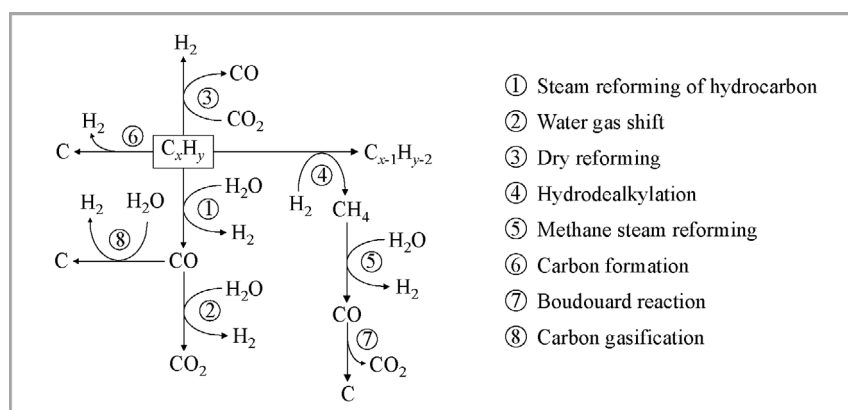


Fig. 4 Possible reaction pathways for steam reforming of tar.

Table 3 Summary of catalytic gasified biomass tar steam reforming processes

Active metals	Supports	Preparation methods	Tar model compound	Operating conditions	Catalytic performance/%	Remarks	Ref.
Ni (10% (wt.))	Activated char	Impregnation	Toluene, naphthalene	$T = 800^{\circ}\text{C}$, S/C = 2, GHSV = 8000 h^{-1}	Tar conv. = 92–100, H ₂ comp. = 66–67	Structural damage and surface area deterioration were observed on spent catalyst	[41]
Ni (10% (wt.))	Al ₂ O ₃ , MgO, CaO	–	Toluene, phenol, naphthalene, pyrene	$T = 450^{\circ}\text{C}$, S/C = 5, GHSV = 1900 h^{-1}	Tar conv. = 80–100, H ₂ yield = 2–13	Ni/Al ₂ O ₃ and Ni/CaO had an unstable behavior in H ₂ yield	[79]
Ni (20% (wt.))	Al ₂ O ₃	Impregnation	Phenol, toluene, Furfural, methyl naphthalene, ndene, anisole	$T = 750^{\circ}\text{C}$, S/C = 3	C conv. = 90, H ₂ yield = 14.3	H ₂ yield is much lower than the potential H ₂ yield (63%) calculated from stoichiometry; O ₂ contributed the largest constitute of reformat followed by CO and H ₂	[24]
Cu (1% (wt.))	Calcined scallop shell	Incipient wetness impregnation	Tar derived from cedar wood gasification	$T = 700^{\circ}\text{C}$, Catalyst = 2 g, Water = 0.09 mL/min	H ₂ yield = 60 mmol/g _{carbon}	Existence of Ca(OH) ₂ on catalyst improved the basicity of catalyst and anti-coking ability	[84]
Ru (1% (wt.))	12SrO-7Al ₂ O ₃	Physical mixing, impregnation	Toluene	$T = 600^{\circ}\text{C}$, S/C = 2, W/F = 7 g h/mol	Tar conv. = 80	Ru(PPh ₃) ₃ Cl ₂ recognized as a better Ru precursor for a high catalytic activity as compared with RuCl ₃ \cdot nH ₂ O	[87]
Pt (1.5% (wt.))	Al ₂ O ₃ , CeO ₂ /Al ₂ O ₃	Incipient wetness impregnation	Toluene	$T = 700^{\circ}\text{C}$, Steam/toluene = 40	Tar conv. = 80–95, H ₂ comp. = 65–68, H ₂ /CO = 6.5–8.5	Doping of CeO ₂ decreased the selectivity to CO but increased the selectivity to CO ₂ ; Pt/CeO ₂ /Al ₂ O ₃ produced a higher H ₂ /CO	[44]
Ba/Ni, Sr/Ni, Ca/Ni (2.28 + 5% (wt.))	LaAlO ₃	Pechini method /Impregnation	Toluene	$T = 600^{\circ}\text{C}$, S/C = 2, WHSV = 27.1 h^{-1}	C conv. = 28–44, H ₂ yield = 26–41	Toluene conversion and H ₂ yields increased drastically by the addition of alkaline-earth metals	[97]

(Continued)

Active metals	Supports	Preparation methods	Tar model compound	Operating conditions	Catalytic performance/%	Remarks	Ref.
Ni/Ru-Mn (16 + 0.6 + 2.6% (wt.))	α -Al ₂ O ₃	Incipient wetness impregnation	Toluene	$T = 600^{\circ}\text{C}$, S/C = 25, GHSV = 10000 h ⁻¹	C conv. = 100, H ₂ comp. = 68.1	Formation of filamentous carbon which leads to reactor clogging and pressure drop was observed on spent catalyst surface	[45]
Fe (10 wt.%) Fe-Ni (5 + 5 wt.%)	Olivine	Thermal fusion	Toluene	$T = 850^{\circ}\text{C}$, S/C = 0.93, WHSV = 0.88 h ⁻¹	Tar conv. = 98, H ₂ yield = 88-98	Tendency of carbon formation of Fe/olivine was slightly higher than Fe-Ni/olivine	[42]
Pt/Ni (0.85 + 5 wt.%)	La _{0.7} Sr _{0.3} AlO _{3-δ}	Pechini method/ Impregnation	Toluene	$T = 600^{\circ}\text{C}$, S/C = 8.9, GHSV = 12000 h ⁻¹	C conv. = 59.1, H ₂ yield = 52.7	Pt/Ni was the best impregnation order lead to a high H ₂ yield and a high tolerance to coking	[111]
Ni, Co (10 wt.%) Ni/Co (5 + 5 wt.%)	ZrO ₂	Impregnation	Phenol	$T = 600^{\circ}\text{C}$, S/C = 9, WHSV = 115.56 h ⁻¹	Tar conv. = 33-53, H ₂ yield = 24-51	Bimetallic catalyst exhibited better catalytic activity than monometallic catalysts	[117]
Ni (20 wt.%)	Lignite char, Al ₂ O ₃	Ion exchange	Toluene	$T = 650^{\circ}\text{C}$, S/C = 2	H ₂ yield = 512-1125 mmol/g-Ni	Lignite char is readily gasified and not suitable service as catalyst support for steam reforming	[120]
Ni (10 wt.%)	Activated carbon, olivine, Al ₂ O ₃	Incipient wetness impregnation	Toluene	$T = 600^{\circ}\text{C}$, S/C = 2, LHSV = 0.87 h ⁻¹	C conv. = 18-100	The large surface area and micropor- ous structure of activated carbon support contributed to a fine Ni particle distribution and consequently lead to a high catalytic activity	[122]
LaNi _{0.5} Mn _{0.5} O ₃		Pechini method	Toluene	$T = 700^{\circ}\text{C}$, S/C = 3, HSV = 20000 h ⁻¹	Tar conv. = 100, H ₂ comp. = 42	Catalyst required high reduction temperature (up to 1000°C)	[133]
V (3 wt.%)	Mg/Al	Co-precipitation /Impregnation	Toluene	$T = 500^{\circ}\text{C}$, S/C = 2, WHSV = 16.6 h ⁻¹	C conv. = 77.5, H ₂ comp. = 57	A higher V content presented a better activity in toluene conversion while a lower V content produced a higher H ₂ composition of reformate	[138]

Notes: GHSV—gas hourly space velocity; WHSV—weight hourly space velocity; LHSV—liquid hourly space velocity; W/F—time factor (catalyst weight/toluene molar flow rate); C conv.—carbon conversion; Tar conv.—tar conversion; H₂ comp.—H₂ composition

Moreover, the nickel nitrate precursor is more readily reduced to the metallic state, which is important in bond cleavage during steam reforming [81]. In another study, Park et al. [82] also reported that the catalysts derived from nickel nitrate were more stable and active than the catalysts

derived from nickel chloride or nickel sulphide. Although they compared the Ni precursor for catalyst preparation, no explanation was given on how the Ni precursor affected the characteristic of the catalyst, which subsequently influenced the catalytic activity.

Vivanpatarakij et al. [79] conducted a series of tar steam reforming experiments (toluene, phenol, naphthalene and pyrene) at different Ni loadings (10%–20% (wt.)) and Ni-based catalyst supports including Al_2O_3 , MgO , and CaO . Among the support materials used, Al_2O_3 exhibited a higher reactivity in carbon conversion and H_2 production. Based on Ni loading, it was found that stable and near complete conversion occurred for all tar components (except naphthalene) when 20% (wt.) of Ni was loaded on Al_2O_3 . Furthermore, they reported that the tar reforming ability was in the order: naphthalene < pyrene < phenol < toluene.

Kim et al. [83] stated that the formation of spinel NiAl_2O_4 in a higher Ni loading catalyst promotes the formation of carbon on the catalyst and consequently deactivates the catalyst. Artetxe et al. [24] conducted an experiment on the steam reforming of tar compounds (toluene, phenol, anisole, methylnaphthalene, furfural, and indene) over the $\text{Ni}/\text{Al}_2\text{O}_3$ catalyst with a 5%–40% (wt.) of Ni content. They claimed that the optimum Ni loading was 20% (wt.) beyond which the catalytic activity did not increase with further increase in Ni-content in the catalyst. This result can be associated with the formation of larger Ni particles, reduction in the specific surface area, and unreacted carbon on the catalyst surface. From the experiment conducted by Artetxe et al. [24], it can be noticed that oxygenated hydrocarbon have a higher reactivity toward conversion and H_2 production compared to an aromatic hydrocarbon, although oxygenates promote the coke deposition on the catalyst.

4.2 Other metal-based catalysts

Kaewpanha et al. [84] investigated the steam reforming of tar from cedar wood gasification over $\text{Cu}/\text{calcined scallop shell}$ catalysts with different Cu loadings (0.5%–5% (wt.)). They observed that the highest H_2 yield was achieved at a Cu loading of 1% (wt.), while a further increase in Cu loading deteriorated the catalytic performance. This was attributed to the existence of portlandite ($\text{Ca}(\text{OH})_2$) on the 1% (wt.) $\text{Cu}/\text{calcined scallop shell}$ catalyst, which improved the basicity of catalyst and the efficiency of coke suppression. Besides, the CaO contained in the calcined support was reported as CO_2 sorption to shift the water-gas shift (WGS) thermodynamic equilibrium to the H_2 product [85,86]. Therefore, a high Cu loading favored the formation of calcium copper oxide that reduced the amount of CaO on support, consequently reducing the H_2 yield from WGS reaction.

The effect of Ru precursor and pre-treatment conditions (N_2 or H_2 atmosphere) on steam reforming of toluene was investigated by Iida et al. [87]. Two types of precursors, $\text{Ru}(\text{PPh}_3)_3\text{Cl}_2$ by physical mixing and $\text{RuCl}_3 \cdot n\text{H}_2\text{O}$ by impregnation, were employed to prepare the $12\text{SrO}-7\text{Al}_2\text{O}_3$ supported catalysts. It was observed that the catalyst synthesized by physical mixing of $\text{Ru}(\text{PPh}_3)_3\text{Cl}_2$

and N_2 pre-treatment before the steam reforming process exhibited a higher toluene conversion. This finding was explained by the lower melting point of $\text{Ru}(\text{PPh}_3)_3\text{Cl}_2$ (159°C), which further enhanced dispersion over the surface of catalyst support during calcination. Concerning pre-treatment, an inert atmosphere was favored for the reduction of Ru to avoid the sintering of Ru particles compared to the rapid reduction by H_2 stream.

The effect of CeO_2 promoter on toluene steam reforming over $\text{Pt}/\text{Al}_2\text{O}_3$ was evaluated by Castro et al. [44]. The main products of the experiments were H_2 , CO and CO_2 . The results indicated that the $\text{Pt}/\text{CeO}_2/\text{Al}_2\text{O}_3$ catalyst had a lower selectivity toward CO and a higher selectivity toward CO_2 compared to the $\text{Pt}/\text{Al}_2\text{O}_3$ catalyst. This is due to the oxygen vacancies in CeO_2 , which promoted the WGS reaction and oxidation of CO [88,89]. Although CeO_2 promoted catalyst exhibited an excellent activity and a H_2 selectivity, the particles of CeO_2 and Pt were unstable, aggregated, and subsequently deactivated over the reaction time [90,91]. Therefore, future studies on the modification of $\text{Pt}-\text{CeO}_2$ catalyst are required to stabilize the CeO_2 and Pt particles for more effective catalytic activities.

4.3 Promoted catalysts

Promoters are typically employed to modify the support structure of catalysts. This enhances the surface area available for catalytic reaction, the catalytic activity per unit surface area, and stability against unwanted side reactions [92]. Oh et al. [45] performed steam reforming of toluene over Ru-Mn promoted $\text{Ni}/\text{Al}_2\text{O}_3$ catalyst. The $\text{Ni}/\text{Ru}-\text{Mn}/\text{Al}_2\text{O}_3$ catalyst showed a complete carbon conversion at 600°C , with H_2 as the highest fraction of reformat. The reason for this is that the addition of Mn promoter favored the dehydration of the reactant and promoted the C-O and C-C bonds rupture, which resulted in increased H_2 selectivity [93]. Furthermore, the addition of Ru promoter ensured that the spent catalyst had no significant change in Ni crystallite size by sintering, whereas the amorphous carbon deposition was nearly undetected [45,94]. In addition, the high intrinsic kinetics of carbon gasification on Ru and the low carbon solubility in the bulk of Ru prevent carbon growth during steam reforming [95,96].

Toluene steam reforming was conducted by Higo et al. [97] to study the promoting effect of alkaline-earth metals (Sr, Ba, and Ca) on Ni/LaAlO_3 catalyst. The authors reported that the promoting effect is in the order of $\text{Ba} > \text{Ca} > \text{Sr}$ in terms of H_2 yield and carbon conversion. Conversely, the coke formation of catalysts exhibited an opposite trend to the catalytic activity. The catalysts with strong basicity had a high catalytic activity and a high resistance against coke deposition during steam reforming [98–100]. In addition, the alkaline-earth metals neutralized the acidity of catalysts and consequently improved their anti-coking ability by facilitating carbon gasification with

steam. Apart from the basicity property, Ba (which demonstrated the greatest promoting effect) also improved the reducibility of NiO by adsorbing and providing OH derived from steam to Ni active site for carbon decomposition [101].

4.4 Bimetallic or alloy catalysts

As reported, Ni catalysts are prone to coke deposition [79,102] and agglomeration [77,103]. Recently, bimetallic catalyst has been utilized for steam reforming due to its positive effect on metal interactions either through geometric or electronic effects [104]. Therefore, alloying Ni with other metals may improve the coke resistance, stability, and robustness of the catalyst [105–107]. Meng et al. [42] comparatively investigated the activity of Fe-, Fe₂O₃-, and Fe/Ni-based olivine catalysts for toluene steam reforming. Among the catalysts, Fe-Ni/olivine had a higher H₂ yield and resistance to coke formation owing to the synergistic effect of the Fe-Ni alloy particles [108]. Fe has a higher oxygen affinity and provides an oxygen atom to the Ni species to facilitate the decomposition of deposited carbon [109,110]. However, Fe₂O₃/olivine had a slightly higher toluene conversion due to its main oxidized component (Fe₂O₃), which was more readily reduced than MgFe₂O₄.

Mukai et al. [111] reported that Pt/Ni/La_{0.7}Sr_{0.3}AlO_{3-δ} had a high catalytic performance and a low coke deposition for H₂ production via toluene steam reforming. They also stated that the catalytic activity of the catalyst without pre-reduction was almost identical to its pre-reduction variant. This indicated that the additive Pt formed the Pt-Ni alloy structure and permitted rapid reduction of NiO by enhancing the spillover of atomic H on NiO surface through rapid dissociation of H₂ [112,113]. Hence, the synergy between Pt with high reducibility and Ni with a high reforming activity leads to a better performance of the bimetallic catalyst in steam reforming compared to the monometallic catalyst. Mukai et al. [111] also found that the Pt-Ni alloy structure with a better metal dispersion reduced the risk of coke deposition on the catalyst surface, as corroborated by other researchers [114–116].

Nabgan et al. [117] developed a bimetallic NiCo/ZrO₂ catalyst for phenol steam reforming. They observed that the bimetallic catalyst showed a better activity for phenol conversion and H₂ yield compared to the monometallic catalyst. Based on their study, the Ni/ZrO₂ catalyst was deactivated mainly by moisture adsorption and coking. However, by introducing Co to the Ni/ZrO₂ catalyst, the adsorption of moisture was subsequently inhibited. Besides, they also suggested that the bimetallic catalyst neutralized the acidity of catalyst, whereas the monometallic catalyst promoted the acid properties of the catalyst. Moreover, a study on NiCo/Al₂O₃ by Luo et al. [118] revealed that an increase in Co loading resulted in a high H₂ selectivity and a low CH₄ production during

glycerine steam reforming. The synergy between Ni and Co also improved the anti-metal sintering ability of catalyst due to the formation of Ni-Co alloy, stable solid solution, and strong metal-support interaction [119].

4.5 Catalyst support

Cao et al. [120] conducted a steam reforming of toluene over Ni/Al₂O₃ and Ni/lignite char catalysts at 650°C. They stated that the catalytic performance and deactivation were related to the support. The Ni/Al₂O₃ had a stable performance for 5 h without particle sintering but with a low amount of carbon deposited on the catalyst. Conversely, Ni/lignite char was rapidly deactivated by Ni particle aggregation. This is attributed to the structural destruction of carbon support by steam gasification. Therefore, Ni/lignite char catalyst is not suitable for steam reforming although it had an excellent anti-coking ability. Although the Ni/Al₂O₃ has stable performance, in this case, the Ni/Al₂O₃ catalyst is always reported with rapid deactivation. For example, Park et al. [121] found that Ni/Al₂O₃ showed a severe catalytic deactivation after 30 h of reaction. Therefore, in this case, 5 h of the catalytic test failed to provide adequate proof for the stability of the catalyst.

Liu et al. [122] evaluated the activity of Ni-based catalyst with different supports for the steam reforming of toluene. It was found that activated carbon provided a large surface area and a microporous structure to generate a catalyst with fine Ni particles and a high Ni dispersion. On the other hand, the low surface area of olivine causes the sintering of Ni during calcination and steam reforming reaction. Although Al₂O₃ has a larger surface area, it is prone to deactivation by coke deposition compared to activated carbon and olivine. They concluded that the Ni/activated carbon catalyst exhibited the highest carbon conversion and stability. Unlike the findings of Cao et al. [120], the carbon in the lignite char was readily gasified during steam reforming. However, the gasification of the activated carbon support was very low but did not diminish its catalytic activity during steam reforming. The Al₂O₃ and olivine supported catalysts were, however, not as effective as activated carbon supported catalyst, particularly the olivine supported catalyst.

Ni/Al₂O₃ and Ni/olivine catalysts initially showed a lower activity, which was ascribed to the incomplete reduction of Ni oxide [122]. Furthermore, the strong interaction of the active metal and support severely hindered reduction. For example, the formation of spinel NiAl₂O₄ after calcination had a high resistance against reduction and may be reduced at a temperature of above 800°C [123,124]. In this case, the Ni/olivine catalyst was calcined at 1000°C followed by a reduction at 700°C. As reported by other researchers [125–127], a high-temperature calcination (900°C–1400°C) causes the replacement of Mg in the olivine lattice by Ni. The strong Ni-olivine

interaction requires high temperatures for full reduction of NiO species (900°C–950°C) [125–127]. Due to the smaller pore volume and surface area, the Ni/olivine catalyst experienced a fast deactivation by pore clogging. However, the acidic support of Ni/Al₂O₃ catalyst promoted the formation of coke on the acid sites through the oligomerization of the toluene molecule [44].

The various textural, acid-basic, and potential metal-support interaction properties of supports are a crucial element in the preparation of catalysts with a high stability and activity [128,129]. The temperature of calcination and reduction which dominate the transformation of metal precursor to active metallic phase is also an essential factor for catalyst preparation. Thermogravimetric analysis and temperature-programmed reduction techniques are proposed to determine the suitable temperature for calcination and reduction, respectively. Other characterization techniques can also be integrated with these thermal analyses to investigate the physical and chemical changes of catalyst.

4.6 Perovskite and hydrotalcite catalysts

Perovskite (ABO₃, where A = alkaline earth metal or lanthanide; B = transition metal such as Mn, Ni, Co, and Cu) could either be a catalyst or a support for the active metal. Typically, the A-site metal has a powerful effect on stability while the B-site metal represents the primary active site [130]. Typically, perovskite has an excellent thermal stability, a well-defined structure, and mobile oxygen, which are beneficial to steam reforming reaction [131,132].

The perovskite catalyst LaNi_{0.5}Mn_{0.5}O₃ was developed and investigated by Quitete et al. [133] for toluene steam reforming. The catalyst accomplished the complete conversion of toluene at 700°C and an S/C ratio of 3, which is close to industrial-scale values. Despite its low specific surface area (1.9 m²/g), LaNi_{0.5}Mn_{0.5}O₃ showed an active and stable behavior in toluene steam reforming for 22 h of reaction. As reported [98,134,135], Ni-based perovskite catalysts are relatively stable and resistant to deactivation by coking.

Hydrotalcite, also known as an aluminum-magnesium layered double hydroxide, is a naturally occurring nanostructured anionic clay. It has high thermal stability and provides a large surface area for uniform dispersion of active metals [136,137]. Compared to alumina supported catalysts, hydrotalcites are more resistant to metallic sintering and coke formation [137].

Mitran et al. [138] studied the effect of vanadium loading (0.9%–3% (wt.)) on the steam reforming of toluene. They observed that V/MgAl catalysts that contain polyvanadate species are more active during steam reforming of toluene. However, the catalysts with isolated species possess a higher selectivity for H₂ production. For a higher loading of V in the catalyst, the monometric VO_x (i. e., V-O-support) is the predominant species that can be

reduced at higher temperature [139,140]. For a lower loading of V in the catalyst, the polymetric VO_x (i. e., V-O-V, which has less interaction with support) is the pronounced species that can be reduced at a lower temperature [139,140]. Other studies also claim the addition of V promotes the WGS activity [139,141], but the H₂ constitution of reformat does not show a linear correlation with its loading [141] due to the side reaction of steam reforming.

Table 4 shows the comparison of perovskite and hydrotalcite catalysts with conventional supported catalysts (discussed in Section 4.4). It can be concluded that perovskite and hydrotalcite catalysts have a more complex structure and better properties compared to conventional supported catalysts. The unique structure of perovskite improves the dispersion of transition metals and offers a stable interaction within the perovskite lattice [142]. However, calcined hydrotalcite with a small crystal size offers a highly specific surface area for good dispersion of active sites [143]. Besides, the redox property of perovskite with high mobility of lattice oxygen promotes the oxidation of deposited coke [144]. Therefore, perovskite and hydrotalcite catalysts have a better performance in terms of catalytic activity, coke suppression, and thermal stability [144].

5 Parametric effect on steam reforming of gasified biomass tar

From previous literature studies, the most important factors for tar steam reforming are temperature, S/C ratio, and space velocity or space time [145,146]. In this section, the effect of these factors on steam reforming efficiency is presented. The favored conditions of gasified biomass tar steam reforming for H₂ production are summarized in Tables 5 to 7.

5.1 Temperature

The reaction temperature has a significant impact on steam reforming of gasified biomass tar and the catalyst used. At a higher temperature, the endothermic steam reforming reaction is enhanced, thereby resulting in thermodynamic equilibrium displacement of the exothermic WGS reaction. Consequently, maximum conversion occurs, resulting in higher yields of H₂ [49,147,148].

Josuinkas et al. [74] examined the influence of temperature on the steam reforming of benzene, toluene, and 10% (wt.) naphthalene/toluene over Ni/MgO/Al₂O₃ catalyst. It was found that the most favorable temperature for complete conversion of benzene and toluene was 700°C. However, naphthalene was more resistant to conversion even at high temperatures. In the steam reforming of naphthalene/toluene, toluene was inhibited by naphthalene and the favorable temperature for complete

Table 4 Comparison of perovskite and hydrotalcite catalysts with conventional supported catalysts

Catalyst	Perovskite	Hydrotalcite	Conventional supported
General formula	ABO ₃ where A = alkaline earth metal; B = transition metal	Mg ₆ Al ₂ CO ₃ (OH) ₁₆ ·4(H ₂ O)	Metal oxide, oxides mineral, carbonaceous material
Examples of Ni based catalyst	LaNi _{0.5} Mn _{0.5} O ₃ , La _{0.9} Ni _{0.2} Mg _{0.1} Al _{0.8} O ₃	Ni/MgAl	Ni/Al ₂ O ₃ , Ni/olivine, Ni/lignite char
Structure	Crystal structure, nonstoichiometric oxygen	Brucite-like structure, where Mg ²⁺ attached with OH ⁻ ions to form octahedral structure	—
Synthesis method	Complex, i.e., citrate method, solution combustion techniques	Complex, i.e., urea hydrolysis, sol-gel method, microwave treatment	Easier, i.e., impregnation, precipitation
Thermal stability	Higher	Higher	Lower especially carbonaceous material
Resistance against coke deposition	Stronger	Stronger	Weaker

Table 5 Favored temperature for H₂ production in steam reforming of gasified biomass tar

Favored temp. /°C	Tar model	Catalyst	Metal loading /% (wt.)	Other operating condition	Catalytic performance/%	Remark	Ref.
700–900	Toluene, toluene/naphthalene	Ni/MgO/Al ₂ O ₃	10.0	S/C = 1.5, GHSV = 20000 h ⁻¹	Tar conv. = 89–100, H ₂ comp. = 22–30	CO ₂ and CO are the main products at lower and higher temperatures, respectively; large cyclic HCs have a higher thermal stability	[74]
800	Toluene	Ru/α-Al ₂ O ₃ , Ni/α-Al ₂ O ₃	2.0	S/C = 3.57, WHSV = 10000 h ⁻¹	C conv. = 96–98, H ₂ comp. = 69–76	Ru is more stable and has a higher activity toward tar conversion than Ni	[121]
800	Phenol	Ni/γ-Al ₂ O ₃	10.0	S/C = 13, WHSV = 0.444 h ⁻¹	C conv. = 57, H ₂ comp. = 14	The low conversion may be due to the use of the unreduced catalyst	[31]
650–750	Toluene	Ce _{0.4} Ni _{0.6} AlO ₃ , La _{0.2} Ni _{0.8} AlO ₃	5.8	S/C = 1.5, WHSV = 23068 h ⁻¹	Tar conv. = 100, H ₂ comp. = 25–30	The present of CeO ₂ allows the full conversion of toluene at a lower temperature	[150]

Notes: WHSV—weight hourly space velocity; C conv.—carbon conversion; Tar conv.—tar conversion; H₂ comp.—H₂ composition

Table 6 Favored S/C ratio for H₂ production in the steam reforming of gasified biomass tar

Favored S/C ratio	Tar model	Catalyst	Metal loading (wt.%)	Other operating condition	Catalytic performance (%)	Remark	Ref.
3.5–5.0	Toluene	Ni/olivine, Ni/Ce/olivine, Ni/Ce/Mg/olivine	3.0	T = 790°C, GHSV = 782	C conv. = 59–93, H ₂ comp. = 60–66	Ni/Ce/Mg/olivine had a more stable performance at a low S/C ratio	[158]
2.0	Benzene	NiO/ceramic foam	3.5	T = 750°C, WHSV = 5.6	C conv. = 85.4, H ₂ comp. = 60	The H ₂ selectivity is not affected by S/C ratio in this case	[156]
8.0	Phenol/ethanol	Ni/Cu/sepiolite clay	20.0	T = 650°C, WHSV = 3.2	C conv. = 75, H ₂ yield = 73	The limit of S/C ratio is not achieved since carbon conversion showed an increased trend	[159]

Notes: GHSV—gas hourly space velocity; WHSV—weight hourly space velocity; C conv.—carbon conversion; H₂ comp.—H₂ composition

Table 7 Favored space velocity or space time for H₂ production in steam reforming of gasified biomass tar

Favored WHSV/h ⁻¹	Tar model	Catalyst	Metal loading/% (wt.)	Other operating condition	Catalytic performance/%	Remark	Ref.
5000	Toluene	Ru/ α -Al ₂ O ₃	2.0	$T = 700^{\circ}\text{C}$, S/C = 1.43	Tar conv. = 87.4, H ₂ comp. = 61.5	Carbon conversion showed a decreased trend with space velocity, indicating that the adsorption-limited was not achieved	[121]
10000	Toluene	Ni/coal	10.6	$T = 400^{\circ}\text{C}$, S/C = 15	H ₂ yield = 62	H ₂ yield was stabilized above 40000 h ⁻¹ , implying that the adsorption-limited was achieved	[163]
0.1–0.4	Toluene, benzene, phenol	Ni/Mg/Al, Ni-Fe/Mg/Al	12.0	$T = 600^{\circ}\text{C}$, S/C = 1.67	Tar conv. = 100%, H ₂ /CO = 4.4–5.6	Ni-Fe alloy has a better performance than Ni-based catalyst although Ni based catalyst showed a higher H ₂ /CO ratio of reformat	[109]

Notes: Tar conv.—Tar conversion; H₂ comp.—H₂ composition

conversion increased to 900°C. This finding is in good agreement with Qian et al. [41] and Jess [149]. Since naphthalene and heavier HCs (e.g., 2–4 rings) typically constitute around 33%(wt.) in gasified biomass tar [62], the less reactivity of heavier HCs reforming should be taken into account. Although toluene could completely be converted at 900°C when mixed with naphthalene, the temperature is too high which limits the application in the industry in terms of cost and safety. Therefore, more broad research is required to determine more effective catalyst and suitable operating conditions for steam reforming of tar.

Park et al. [121] examined the steam reforming of toluene over Ru- and Ni-based catalysts supported on α -Al₂O₃ at different temperatures. They pointed out that the H₂ selectivity and toluene conversion of both catalysts increased dramatically with elevating reaction temperature. Artetxe et al. [31] reported similar observations. Similarly, Quitete and Souza [150] investigated the steam reforming of toluene over perovskite catalysts from 400°C to 800°C. They observed that Ce_{0.4}Ni_{0.6}AlO₃ had a better catalytic performance and achieved complete toluene conversion at 650°C whereas La_{0.2}Ni_{0.8}AlO₃ exhibited complete conversion at 750°C. This can be attributed to the high oxygen-release capacity of CeO₂, which strongly inhibits coke deposited on the catalyst, consequently reducing the risk of catalyst deactivation (Fig. 5) [151,152].

5.2 Steam to carbon ratio

The S/C ratio is one of the crucial factors in steam reforming of gasified biomass tar due to its impact on coke formation, feedstock conversion, and H₂ yield [153,154]. The increase in the S/C ratio reduces coke formation by facilitating the gasification of deposited carbon, as verified by Tao et al. [155]. The authors performed an elemental analysis, which indicated that the carbon content of the

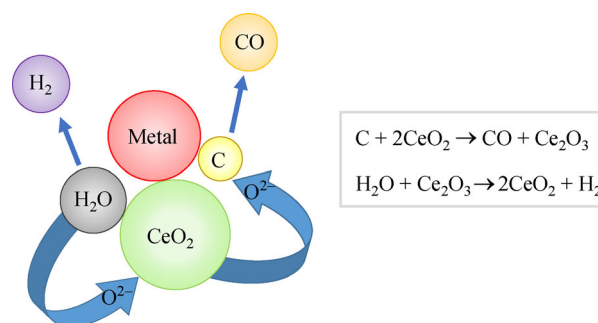


Fig. 5 Mechanism of coke suppression by CeO₂ support.

spent catalyst decreased at higher S/C ratios. However, excess steam negatively influenced the tar conversion since water molecules competed with tar at adsorptive active sites. This was verified by Gao et al. [156] who conducted benzene steam reforming over Ni/ceramic foam catalyst with a distinct S/C molar ratio (0–3). Furthermore, the high S/C ratio is not feasible for industrial application because of the associated cost of high power consumption for steam generation and steam separation from the reformat. Excess steam also absorbs the heat within the reactor, which leads to a fluctuation in the reaction temperature [157]. On the other hand, insufficient steam supplement causes the steam reforming and WGS reactions cannot achieve their state of completion, consequently resulting in the low conversion and H₂ production [157]. Therefore, the S/C molar ratios used in the reaction should be higher than the stoichiometric value of the reaction

Zhang et al. [158] studied the effect of S/C ratio on toluene steam reforming over Ni-based catalysts and concluded that H₂ composition increased as S/C ratio increased. However, the result was not consistent with the findings of Gao et al. [156], which showed a stable trend of H₂ composition at a higher S/C ratio. Similarly, Zhang et al. [158] also observed that the highest carbon

conversion was obtained at an S/C ratio of 5 with Ni and Ni/Ce based olivine catalysts while at an S/C ratio of 3.5 with Ni/Ce/Mg/olivine catalyst. The addition of Mg to Ni/Ce/olivine enhanced the performance and coke resistance at the S/C ratio of 3.5. This is due to its basicity and the presence of well-stabilized NiO-MgO solid solution. Liang and coworkers [159] investigated the effect of different S/C ratios on steam reforming of phenol-ethanol over bimetallic Ni-Cu/sepiolite catalyst. The results demonstrated that H₂ yield and carbon conversion increased with rising S/C ratios. This is because sufficient steam drives the tar reforming and a high water partial pressure favors the equilibrium of WGS reaction shift toward H₂ production [121,159].

5.3 Space velocity and space-time

Catalytic steam reforming is influenced by the space velocity and space-time, which reflects the contact time of tar on the active sites of the catalyst [160,161]. The variables are significant to avoid catalyst from wastage during industrial applications. When the adsorption sites of a catalyst are limited, the chemical reaction rate is less sensitive to space velocity and space-time [31]. With regard to space-time, tar conversion increases as space-time are increased, which indicates that the active sites of the catalyst increases or the contact time of the tar-active sites increases [162].

Park et al. [121] studied the steam reforming of toluene over Ru/ α -Al₂O₃ with a space velocity ranging from 5000 to 30000 h⁻¹. They observed that carbon conversion and H₂ production were inversely proportional to the space velocity. In another study, the variation of H₂ yield from toluene steam reforming over Ni/coal with distinct space velocity range was analyzed by Kim et al. [163]. The H₂ yield decreased with increasing space velocities. Koike et al. [109] analyzed the space-time effect on the catalytic performance of tar steam reforming over Ni and Ni-Fe alloy catalyst supported on the Mg-Al hydrotalcite-like material. The results indicated that tar conversion increased with increasing space-time. However, the H₂/CO ratio decreased with increasing space-time. At a higher tar conversion, the residual of H₂O decreased, thereby

limiting the contribution of WGS reaction and H₂ selectivity.

6 Challenges of steam reforming of gasified biomass tar

Although great efforts have been devoted to steam reforming catalyst research, several challenges still exist, including catalyst deactivation, material selection for reactor fabrication, engineering economics and operational cost for high temperature (700°C to 900°C) reactions. Besides the operating costs, the high temperature also affects issues such as catalyst deactivation [164] and sintering [31,77].

6.1 Catalyst deactivation

Typically, Ni-based catalysts are deactivated after a long reaction time, which strongly limits their industrial application [165]. However, the most common deactivation problems include ① coke formation which blocks the active site and encapsulates the metal particles; ② active metal sintering which decreases the exposed surface area of the active site [166,167].

6.1.1 Coke formation

At lower temperatures (<400°C), the reverse of Boudouard reaction (Eq. (8)) and reverse of carbon gasification (Eq. (9)) facilitate the formation of coke on catalyst surface [164]. During steam reforming, coke can deposit on catalyst either as amorphous (Fig. 6(b)) or filamentous carbon (Fig. 6(c)). Note that the former leads to the deactivation caused by the hindrance of the active site, whereas the latter does not significantly contribute to deactivation but causes reactor clogging and pressure depression [74,121,168].

Hu et al. [102] observed that both amorphous (12.76 mg/g_{catalyst}) and filamentous coke (16.84 mg/g_{catalyst}) existed on spent Ni/Al₂O₃ catalyst. These results were verified by temperature-programmed oxidation (TPO) analysis, as presented in Fig. 7. Besides, the addition of Fe contributed

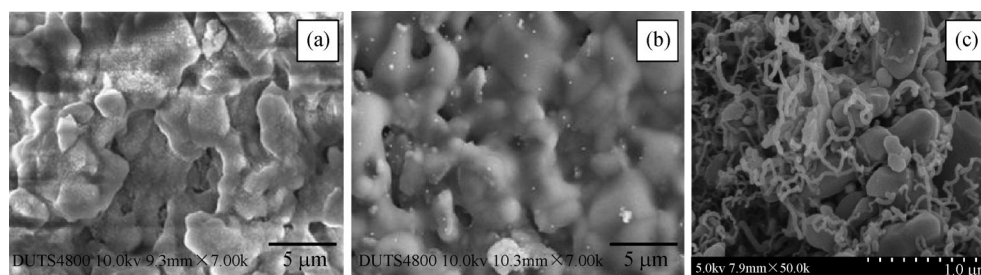


Fig. 6 SEM images of (a) fresh NiO/ceramic catalyst (adapted with permission from Ref. [157]); (b) amorphous coked NiO/ceramic catalyst (adapted with permission from Ref. [157]); (c) filamentous coked Ni/ α -Al₂O₃ catalyst (adapted with permission from Ref. [121]).

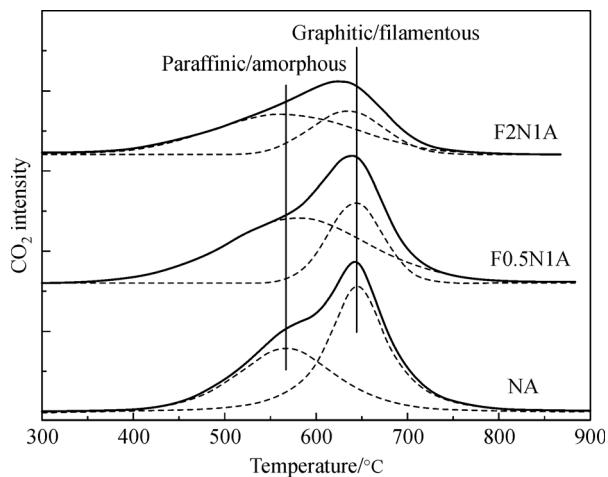


Fig. 7 TPO profiles of spent Ni/Al₂O₃ and Fe-Ni/Al₂O₃ catalysts after steam reforming of toluene (adapted with permission from Ref. [102]).

to coke suppression by increasing the coverage of oxygen species on the catalyst surface. A similar phenomenon has also been observed on the Ni-Fe/SBA-15 catalyst by Kathiraser et al. [169]. In the case of Ru/SrCO₃-Al₂O₃ catalyst, Lida et al. [170] proposed that the amount of coke deposited was remarkably higher with decreasing SrCO₃/Al₂O₃ loading ratio. This is because of the decrease in coke suppression agent, SrCO₃ which possesses a highly reactive hydroxyl functional group. As reported by Karnjanakom et al. [103], the coke formation rate of the Ni/MCM-41 catalyst was sequentially increased with the Ni content (5%–40% (wt.)). The authors showed that the ethylene glycol assisted method enhances the resistance of Ni/MCM-41 to coke deposition compared to the co-impregnation method.

6.1.2 Active metal sintering

The presence of excess steam and high temperature accelerates the sintering rate of the active metal in catalysts [31,77]. For instance, Ni-based catalysts are susceptible to sintering by agglomerating metallic Ni particles since the steam reforming temperature (700°C–900°C) is typically higher than its Tammann temperature (691°C, above which Ni sintering will readily take place) [171,172].

Oemar et al. [135] reported that apart from the coke deposition, the metal sintering of LaNiO₃ catalyst also decreased its catalytic activity (Fig. 8). The Ni crystallite size of spent LaNiO₃ was increased considerably by 34.7% after 8 h of reaction. Park et al. [121] stated that the deterioration of Ru/ α -Al₂O₃ resulted from Ru sintering, which yielded a bulky crystalline structure that was detrimental to further catalytic reactions. Quitete et al. [173] concluded that NiO/CaAl₁₂O₁₉ and NiO/LaAl₁₁O₁₈ with a low Ni loading (approximately 6% (wt.)) experi-

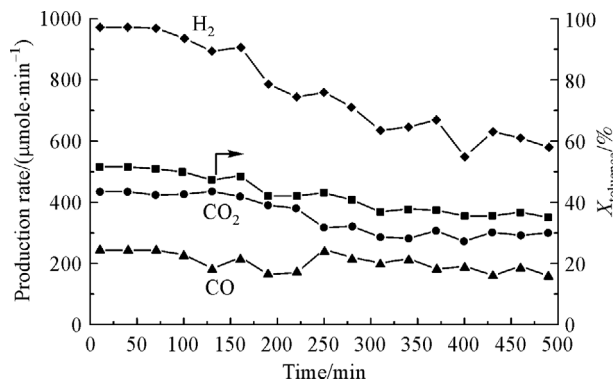


Fig. 8 Activity of LaNiO₃ catalyst. Reaction condition: S/C 3.9; catalyst 0.03 g; temperature 650°C; He 120 mL/min (adapted with permission from Ref. [135]).

enced shrinkage in Ni crystallite size after reduction. Furthermore, the catalysts experienced a rapid sintering-related deactivation (increased above 150% of Ni crystallite size) compared to the high Ni loading catalyst (14% (wt.)) [173]. In contrast, Karnjanakom et al. [103] mentioned that the high loading of Ni in Ni/MCM-41 catalyst (20%–40% (wt.)) promoted not only the coke deposition rate but also the sintering.

6.1.3 Catalyst poisoning

The presence of impurities in the biomass-derived syngas such as sulfur-, nitrogen-, and chlorine containing compounds could poison the catalyst in the downstream tar reforming process [174,175]. Of the impurities, sulfur is the most common poison, causing severe deactivation of steam reforming catalysts. However, apart from the H₂S, the effect of other impurities on the steam reforming of tar has not been extensively investigated. Nitrogen-containing compounds such as nitrogen oxides (NO_x) could deactivate catalyst by oxidizing the active metal [175]. On the other hand, hydrogen chloride (HCl) poisons the catalyst due to the chemisorption of HCl on a metal site followed by metal sintering [174,176]. This process leads to an irreversible deactivation of catalyst and causes an abatement of catalytic activity.

Generally, about 20–200 ppm of sulfur-containing compounds, mainly hydrogen sulphide (H₂S), is contained in the syngas derived from biomass gasification [177–179]. Metal catalysts, especially Ni catalyst, are susceptible to sulfur poisoning due to the strong dissociative chemisorption of sulfur on the metal site [174,180,181]. For example, H₂S chemisorbs on the Ni site, which alters the atomic surface structure and forms inactive nickel sulphide (Eq. (10)) [182,183], consequently reducing the accessibility of active sites for tar. In addition, the presence of H₂S also promotes the coke formation during steam reforming of tar [133,184]. The reason for this is that the formation of

inactive metal sulphides suppresses the reforming reaction while the tar cracking reaction continues to take place, leading to the coke formation that derived from the carbonaceous product of tar cracking [184]. However, the sulfur poisoning can be prevented only at high pressures (20–30 bar) and temperature ($>900^{\circ}\text{C}$) but those conditions are less favorable to the industrial application [185].



6.2 Type and material of the reactor

Catalytic steam reforming is considered as a promising approach for addressing tar formation and improving the H_2 production during biomass gasification. Steam reforming is prone to challenges, which must be eradicated to ensure higher productivity and effective commercialization. Typically, tar contains heavy polycyclic aromatic hydrocarbon with a high thermal stability [74,154]. The steam reforming process requires a high operating temperature (700°C – 900°C). However, the high temperature and internal pressure make the reformer tube susceptible to creep cracking. In principle, the control of high temperatures poses a tough challenge, which increases the operational or capital costs of power consumption, reactor material, engineering, and installation [186,187].

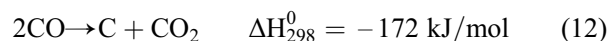
Currently, nickel- or iron-based oxide dispersion strengthened alloys that withstand an extreme temperature of 1100°C are available but relatively expensive [188]. Inconel is nickel-chromium-based superalloys used extensively for reformer tubes in steam reforming [189]. Moreover, refractory metals like tungsten and molybdenum exhibit extremely poor oxidation resistance but provide a high-temperature endurance capability [190]. Superplastic ceramic materials are also one of the acceptable candidates for a high temperature but require further development of appropriate joining methods [188].

Several types of reactors have been employed for steam reforming. The fixed bed reactor is the most common and simplest type for industrial-scale H_2 production. The drawbacks of the fixed bed reactor consist of significant radial and axial temperature gradients that lower the bed effective thermal conductivity [191]. Micro-channel reactor with well-coated catalysts provides a high surface area to volume ratio, which leads to a better heat and mass transfer within the reactor. However, the problem of this reactor is the low durability of the coated catalyst [192]. Besides, the requirement of a well-defined catalyst with a regular shape and much smaller particles limits the application of commercial catalysts [193]. Membrane reactors produce the high purity of particular gas but its fabrication cost is relatively high and the mechanical resistance is low [193]. Therefore, a suitable type and high-

temperature resistance material must be considered in reactor design to balance the trade-off between the safety and economy of the reactor.

7 Dry reforming and its challenges

Typically, 10% to 30% (vol.) of CO_2 is released from the biomass gasification [194]. Therefore, CO_2 reforming of tar toward hydrogen gas, so-called dry reforming of tar (Eq. (4)), was recently developed by some researchers [195–198]. Dry reforming reduces the CO_2 emission, improves the carbon conversion, and eliminates the cost of a steam generation [198]. However, the equilibrium of gas production is generally affected by the reverse WGS reaction (Eq. (10)). This results in the lower H_2/CO ratio of produced gas and is less favorable for hydrogen production [199]. Dry reforming also suffers rapid catalyst deactivation by carbon deposition via CO disproportionation (Eq. (11)). Besides, the adsorption of CO and CO_2 on the catalyst can decelerate the dry reforming rate [200].



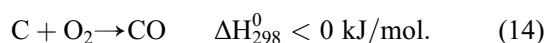
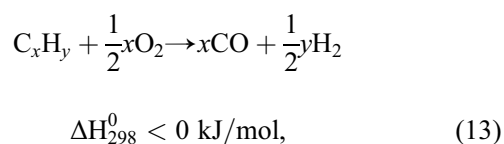
Rached et al. [197] investigated the addition of Ce and La into Ni-Al catalyst for dry reforming of toluene. Ce and La promote the CO_2 adsorption, hinder the CO disproportionation, and consequently reduce the carbon deposition on the active metal [201]. They reported that Ce promoted catalyst had a more pronounced CO_2 adsorption effect and a better resistance against coke formation on the catalyst. Bao et al. [198] evaluated the performance of Co/MgO catalyst in dry reforming of tar at 570°C . They claimed that the activity and stability of the catalyst increased with the loading of Co (5%–15% (wt.)). With the evidence of TGA and XRD analysis of spent catalyst, coke deposition and sintering-related deactivations are negligible in this case. However, they found that the catalyst deactivation was mainly attributed to the oxidation of metallic Co by CO_2 during the dry reforming reaction.

8 Autothermal reforming and its challenges

To address the catalyst deactivation and intensive energy consumption of steam reforming, oxygen (O_2) gas is introduced to promote the cracking reaction and hinder the carbon deposition [202,203]. This process is the so-called autothermal reforming (ATR) or oxidative steam reforming. The involvement of partial oxidation (POX) in ATR also increases the yield of H_2 . By combining the endothermic steam reforming (Eq. (1)) and exothermic POX (Eq. (12)) [204], external heat supply and indirect

heat exchangers are not required by ATR [46]. The reason for this is that, by increasing O_2 to a level, the energy consumption via steam reforming is balanced by the energy generated from the oxidation [205]. Hence, the overall reaction is theoretically autothermal or self-sustaining.

The dominant reactions during ATR are steam reforming, POX, and WGS reactions. ATR also shows a lower coke formation on the catalyst as compared to steam reforming. The oxidative environment allows a portion of deposited coke oxidized by oxygen to produce CO (Eq. (13)). Thus, catalyst can be used for prolonged periods without deactivation [206]. However, ATR either requires a costly O_2 purification system for pure O_2 feeding or treats the product gas with a diluent (N_2 from the air) [205]. However, introducing of air instead of O_2 is typically reported as reducing the heating value of the process.



Wang et al. [202] integrated the $La_{0.8}Sr_{0.2}Ni_{0.8}Fe_{0.2}O_{3-\delta}$ (LSNF) perovskite catalyst with $BaBi_{0.05}Co_{0.8}Nb_{0.15}O_{3-\delta}$ (BBCN) hollow fiber membranes for ATR of toluene (see Fig. 9). They found that the integration offered a higher conversion and a lower carbon deposition than using catalyst only. This is because the oxygen permeable membrane transports lattice oxygen to the steam reforming reaction, consequently provides another form of reforming agent for POX. In this research, the air is introduced to the reactor. The permeable membrane allows only oxygen diffuses through the membrane to reach the catalyst region (see Fig. 10). Therefore, the purity of permeated oxygen can achieve 100%.

9 Future focus and prospect

Since steam reforming is operated at a high temperature, future research on better reactor material and configuration is necessary. In addition, scale-up procedures with highly improved operating temperature control are required to enhance the cost, efficiency, and safety of steam reforming of gasified biomass tar [207]. The CO_2 emissions can be reduced by integrating CO_2 sorbent (e.g. CaO based material) into steam reforming. This is termed the sorption enhanced steam reforming (SESR), which has been examined at the laboratory but not in commercial scale [208–210]. Therefore, further investigation and definite proofs-of-concept for SESR are required to improve the performance of scale-up and industrial scale applications [211,212]. Besides, it is necessary to develop a continuous reaction-regeneration of the SESR system for extended operation time.

The composition of biomass tar is complex, in which, each component has a different influence on reforming efficiency, gaseous product distribution, and catalyst deactivation [24,74,79]. Although recent research studies reported superior catalytic performance in laboratory steam reforming of biomass tar model, the oxygenated and polycyclic aromatic HCs in the real biomass tar could promote coke deposition and lower the activity of the catalyst, respectively. Besides, a matrix of complex reactions among the intermediate products and different tar compositions may occur. It is difficult to predict the catalytic process mechanism during steam reforming of biomass tar. Therefore, it is necessary to conduct research on catalytic performance for steam reforming of real biomass tar to make sure that the coke resistance ability and the activity of the catalyst is adequate to deal with the complex real biomass tar. Besides, a chemical looping system for continuous tar reforming with simultaneous catalyst regeneration is also an important issue for industrial practice.

Moreover, an advanced catalyst with a better catalytic

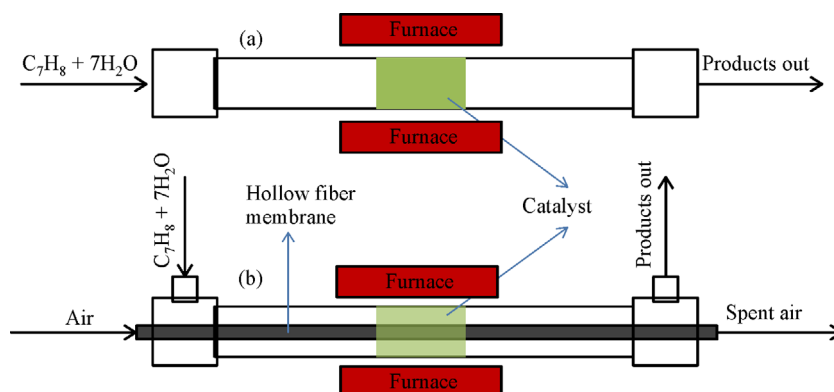


Fig. 9 Schematic diagram.

(a) Catalytic fixed bed reactor; (b) catalytic membrane reactor (adapted with permission from Ref. [202]).

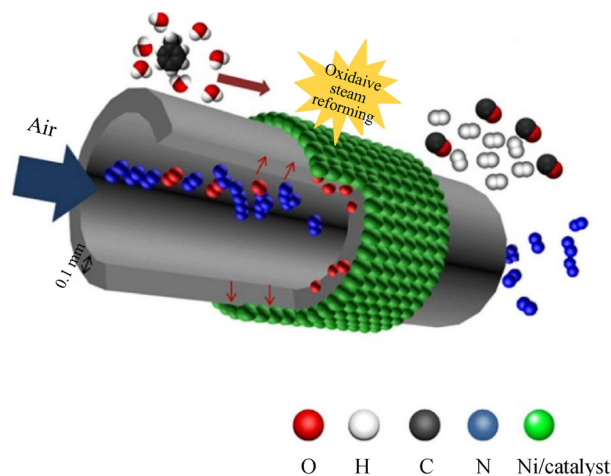


Fig. 10 Steam reforming of toluene in BBCN hollow fiber membrane reactor (adapted with permission from Ref. [202]).

activity, stability, selectivity, and economic feasibility is required for catalytic research and industrialized steam reforming of tar [70,213]. Furthermore, an investigation on the synergetic effect and mutual interaction mechanism of active metal, support, and promoter are recommended in future research, especially, of alloy, hydrotalcite, and perovskite-type catalysts [214,215]. To make the developed catalyst more practical in industrial scale, optimization of tar steam reforming parameters over a newly developed catalyst, for maximum throughput with minimum raw material and energy consumption, merits further examination [145,146,216]. Apart from the conventional steam reforming approach, new technologies such as dry reforming and ATR are desired to be exploited thoroughly and intensively.

To achieve the sustainability of this technology, there are three pillars that must be met, namely, social, environmental, and economic [217]. In the social aspect, the H_2 produced by steam reforming offers alternative energy and reduces the dependence of fossil fuel. In the environmental aspect, steam reforming converts the hazardous tar produced from gasification into H_2 rich gas. The economic aspect indicates that steam reforming is more cost-effective compared to other tar elimination methods because it converts tar into more valuable products and incurs less cost compared to other reforming technologies. Therefore, the improvement of H_2 production by steam reforming of biomass tar complies with the pillars of sustainability. However, the sustainability of this technology can be further improved by CO_2 capture, the application of low-cost element for catalyst preparation, and modified catalyst for high H_2 selectivity.

10 Conclusions

Coking and metallic sintering reactions always occur in

steam reforming of gasified biomass tar. Sometimes, catalyst poisoning also occurs if the gaseous impurities are introduced along with the tar. Despite the significant achievements in catalysis research for tar steam reforming, most catalysts still lack the characteristics to ensure a high feedstock conversion, H_2 selectivity, and the resistance to deactivation. In particular, the investigation of steam reforming of tar along with the raw gaseous products produced from gasification is lacking in the scientific literature. Besides, other desirable qualities, including economic and environmental feasibility, also need to be taken into consideration in effective steam reforming. To obtain an effective catalyst and efficient H_2 production, a combination of suitable catalyst formulation along with proper reactor design and operating conditions plays a significant role. The recent research indicates that promoted, alloy, perovskite, and hydrotalcite-type catalysts have a high potential to enhance the catalytic performance. These catalysts reportedly exhibit a high catalytic activity, a high selectivity toward H_2 , a high stability, and an extended lifetime in tar conversion. Therefore, further research is required to extend the knowledge of this class of catalysts and their operating conditions. On the other hand, the further assessment of the alternative reforming process such as dry reforming and ATR associated with their limitation including costly oxygen purification and catalyst deactivation is essential.

Acknowledgements This work was financially supported by the University Teknologi Malaysia through Research University Grant (GUP Tier 1: 20H52) and by the Universiti Malaysia Perlis through Fundamental Research Grant Scheme (FRGS 9003-00764).

References

1. Nikolaidis P, Poullikkas A. A comparative overview of hydrogen production processes. *Renewable & Sustainable Energy Reviews*,

- 2017, 67: 597–611
- Idrees M, Rangari V, Jeelani S. Sustainable packaging waste-derived activated carbon for carbon dioxide capture. *Journal of CO₂ Utilization*, 2018, 26: 380–387
 - Yaumi A L, Bakar M Z A, Hameed B H. Recent advances in functionalized composite solid materials for carbon dioxide capture. *Energy*, 2017, 124: 461–480
 - Triantafyllidis S, Ries R J, Kaplanidou K K. Carbon dioxide emissions of spectators' transportation in collegiate sporting events: comparing on-campus and off-campus stadium locations. *Sustainability*, 2018, 10(1): 241
 - US Environmental Protection Agency. *Inventory of US greenhouse gas emissions and sinks: 1990–2014*. Washington: US Environmental Protection Agency, 2016
 - Sreenivasulu B, Gayatri D V, Sreedhar I, Raghavan K V. A journey into the process and engineering aspects of carbon capture technologies. *Renewable & Sustainable Energy Reviews*, 2015, 41: 1324–1350
 - Intergovernmental Panel on Climate. *Climate Change 2014: Mitigation of Climate Change*. Cambridge: Cambridge University Press, 2015
 - Berry P, Ogawa-Onishi Y, McVey A. The vulnerability of threatened species: adaptive capability and adaptation opportunity. *Biology (Basel)*, 2013, 2(3): 872–893
 - Abdalla A M, Hossain S, Petra P M, Ghasemi M, Azad A K. Achievements and trends of solid oxide fuel cells in clean energy field: a perspective review. *Frontiers in Energy*, 2018, online, <https://doi.org/10.1007/s11708-018-0546-2>
 - International Energy Agency. *World Energy Outlook 2017*. Paris, France: Organisation for Economic Co-operation and Development, 2017
 - Parthasarathy P, Narayanan K S. Hydrogen production from steam gasification of biomass: influence of process parameters on hydrogen yield—a review. *Renewable Energy*, 2014, 66: 570–579
 - Kalamaras C M, Efstathiou A M. Hydrogen production technologies: current state and future developments. *Conference Papers in Energy*. London, UK: Hindawi Publishing Corporation, 2013
 - Riis T, Hagen E F, Vie P J, Ulleberg Ø. Hydrogen production and storage—R&D: priorities and gaps. *IEA Hydrogen Implementing Agreement*. Paris: International Energy Agency, 2006
 - Dodds P E, Staffell I, Hawkes A D, Li F, Grünwald P, McDowall W, Ekins P. Hydrogen and fuel cell technologies for heating: a review. *International Journal of Hydrogen Energy*, 2015, 40(5): 2065–2083
 - Pei A, Zhang L, Jiang B, Guo L, Zhang X, Lv Y, Jin H. Hydrogen production by biomass gasification in supercritical or subcritical water with raney-Ni and other catalysts. *Frontiers of Energy and Power Engineering in China*, 2009, 3(4): 456–464
 - Moud P H, Kantarelis E, Andersson K J, Engvall K. Biomass pyrolysis gas conditioning over an iron-based catalyst for mild deoxygenation and hydrogen production. *Fuel*, 2018, 211: 149–158
 - Sumrunnonasak S, Tantayanon S, Kiatgamolchai S, Sukonket T. Improved hydrogen production from dry reforming reaction using a catalytic packed-bed membrane reactor with Ni-based catalyst and dense PdAgCu alloy membrane. *International Journal of Hydrogen Energy*, 2016, 41(4): 2621–2630
 - Hosseini S E, Wahid M A, Ganjehkaviri A. An overview of renewable hydrogen production from thermochemical process of oil palm solid waste in Malaysia. *Energy Conversion and Management*, 2015, 94: 415–429
 - Bhattacharyya R, Sandeep K, Kamath S, Mistry K. Hydrogen from alkaline water electrolysis: a case study on process economics of decentralized production in the present Indian scenario. *Emerging Trends in Chemical Engineering*, 2018, 4(3): 1–17
 - Lin M Y, Hourng L W, Huang S H, Tsai T H, Hsu W N. Analysis and study on polarization during water electrolysis hydrogen production. *Chemical Engineering Communications*, 2017, 204(2): 168–175
 - Gu X, Yuan S, Ma M, Zhu J. Nanoenhanced materials for photolytic hydrogen production. *Nanotechnology for Energy Sustainability*, 2017: 629–648
 - Chu K H, Ye L, Wang W, Wu D, Chan D K L, Zeng C, Yip H Y. Enhanced photocatalytic hydrogen production from aqueous sulfide/sulfite solution by ZnO_{0.6}S_{0.4} with simultaneous dye degradation under visible-light irradiation. *Chemosphere*, 2017, 47: 9873–9880
 - Jacobs J D. Economic modeling of cost effective hydrogen production from water electrolysis by utilizing Iceland's regulatory power market. *Dissertation for the Degree of Master of Science*. Iceland: Reykjavik University, 2016
 - Artetxe M, Alvarez J, Nahil M A, Olazar M, Williams P T. Steam reforming of different biomass tar model compounds over Ni/Al₂O₃ catalysts. *Energy Conversion and Management*, 2017, 136: 119–126
 - Chiodo V, Urbani F, Zafarana G, Prestipino M, Galvagno A, Maisano S. Syngas production by catalytic steam gasification of citrus residues. *International Journal of Hydrogen Energy*, 2017, 42(46): 28048–28055
 - Molino A, Chianese S, Musmarra D. Biomass gasification technology: the state of the art overview. *Journal of Energy Chemistry*, 2016, 25(1): 10–25
 - Hosseini S E, Wahid M A. Hydrogen production from renewable and sustainable energy resources: promising green energy carrier for clean development. *Renewable & Sustainable Energy Reviews*, 2016, 57: 850–866
 - Hernández J, Ballesteros R, Aranda G. Characterisation of tars from biomass gasification: effect of the operating conditions. *Energy*, 2013, 50: 333–342
 - Singh R, Singh S, Balwanshi J. Tar removal from producer gas: a review. *Research Journal of Engineering Sciences*, 2014, 3: 16–22
 - Valderrama Rios M L, González A M, Lora E E S, Almazán del Olmo O A. Reduction of tar generated during biomass gasification: a review. *Biomass and Bioenergy*, 2018, 108: 345–370
 - Artetxe M, Nahil M A, Olazar M, Williams P T. Steam reforming of phenol as biomass tar model compound over Ni/Al₂O₃ catalyst. *Fuel*, 2016, 184: 629–636
 - Yoon S J, Choi Y C, Lee J G. Hydrogen production from biomass tar by catalytic steam reforming. *Energy Conversion and Management*, 2010, 51(1): 42–47
 - Nakamura S, Kitano S, Yoshikawa K. Biomass gasification process with the tar removal technologies utilizing bio-oil scrubber and

- char bed. *Applied Energy*, 2016, 170: 186–192
34. Osipovs S, Pučkins A. Choice the filter for tar removal from syngas. In: *Proceedings of the 11th International Scientific and Practical Conference*, Rezekne: Rezekne Academy of Technologies, 2017, 211–215
 35. Choi Y K, Ko J H, Kim J S. Gasification of dried sewage sludge using an innovative three-stage gasifier: clean and H₂-rich gas production using condensers as the only secondary tar removal apparatus. *Fuel*, 2018, 216: 810–817
 36. Woolcock P J, Brown R C. A review of cleaning technologies for biomass-derived syngas. *Biomass and Bioenergy*, 2013, 52: 54–84
 37. Ersoz A, Olgun H, Ozdogan S. Reforming options for hydrogen production from fossil fuels for pem fuel cells. *Journal of Power Sources*, 2006, 154(1): 67–73
 38. McGlocklin K. Economic analysis of various reforming techniques and fuel sources for hydrogen production. Dissertation for the Degree of Master of Science. Auburn: Auburn University, 2006
 39. Myers D B, Ariff G D, James B D, Lettow J S, Thomas C E, Kuhn R C. Cost and performance comparison of stationary hydrogen fueling appliances. In: *Proceedings of the 2002 US DOE Hydrogen Program Review*, Arlington: Directed Technologies, 2002
 40. Forsberg O. Catalytic tar reforming in biomass gasification: tungsten bronzes and the effect of gas alkali during tar steam reforming. Dissertation for the Master Degree. Stockholm: KTH Royal Institute of Technology, 2014
 41. Qian K, Kumar A. Catalytic reforming of toluene and naphthalene (model tar) by char supported nickel catalyst. *Fuel*, 2017, 187: 128–136
 42. Meng J, Zhao Z, Wang X, Wu X, Zheng A, Huang Z, Zhao K, Li H. Effects of catalyst preparation parameters and reaction operating conditions on the activity and stability of thermally fused Fe-olivine catalyst in the steam reforming of toluene. *International Journal of Hydrogen Energy*, 2018, 43(1): 127–138
 43. Takise K, Manabe S, Muraguchi K, Higo T, Ogo S, Sekine Y. Anchoring effect and oxygen redox property of Co/La_{0.7}Sr_{0.3}AlO_{3-δ} perovskite catalyst on toluene steam reforming reaction. *Applied Catalysis A, General*, 2017, 538: 181–189
 44. de Castro T P, Silveira E B, Rabelo-Neto R C, Borges L E P, Noronha F B. Study of the performance of Pt/Al₂O₃ and Pt/CeO₂/Al₂ catalysts for steam reforming of toluene, methane and mixtures. *Catalysis Today*, 2018, 299: 251–262
 45. Oh G, Park S Y, Seo M W, Kim Y K, Ra H W, Lee J G, Yoon S J. Ni/Ru–Mn/Al₂O₃ catalysts for steam reforming of toluene as model biomass tar. *Renewable Energy*, 2016, 86: 841–847
 46. Chen J, Tamura M, Nakagawa Y, Okumura K, Tomishige K. Promoting effect of trace Pd on hydrotalcite-derived Ni/Mg/Al catalyst in oxidative steam reforming of biomass tar. *Applied Catalysis B: Environmental*, 2015, 179: 412–421
 47. Zhao X, Xue Y, Lu Z, Huang Y, Guo C, Yan C. Encapsulating Ni/CeO₂-ZrO₂ with SiO₂ layer to improve its catalytic activity for steam reforming of toluene. *Catalysis Communications*, 2017, 101: 138–141
 48. Heo D H, Lee R, Hwang J H, Sohn J M. The effect of addition of Ca, K and Mn over Ni-based catalyst on steam reforming of toluene as model tar compound. *Catalysis Today*, 2016, 265: 95–102
 49. Zou X, Chen T, Zhang P, Chen D, He J, Dang Y, Ma Z, Chen Y, Toloueinia P, Zhu C, Xie J, Liu H, Suib S L. High catalytic performance of Fe-Ni/palygorskite in the steam reforming of toluene for hydrogen production. *Applied Energy*, 2018, 226: 827–837
 50. Ben-Iwo J, Manovic V, Longhurst P. Biomass resources and biofuels potential for the production of transportation fuels in Nigeria. *Renewable & Sustainable Energy Reviews*, 2016, 63: 172–192
 51. Feng Y, Xiao B, Goerner K, Cheng G, Wang J. Influence of catalyst and temperature on gasification performance by externally heated gasifier. *Smart Grid and Renewable Energy*, 2011, 2(03): 177–183
 52. Kumar A, Jones D D, Hanna M A. Thermochemical biomass gasification: a review of the current status of the technology. *Energies*, 2009, 2(3): 556–581
 53. Li C, Suzuki K. Tar property, analysis, reforming mechanism and model for biomass gasification—an overview. *Renewable & Sustainable Energy Reviews*, 2009, 13(3): 594–604
 54. Guan G, Hao X, Abudula A. Heterogeneous catalysts from natural sources for tar removal: a mini review. *Journal of Advanced Catalysis Science and Technology*, 2014, 1(1): 20–28
 55. Yu H, Zhang Z, Li Z, Chen D. Characteristics of tar formation during cellulose, hemicellulose and lignin gasification. *Fuel*, 2014, 118: 250–256
 56. Marano J J. Benchmarking biomass gasification technologies for fuels, chemicals and hydrogen production. US: National Energy Technology Laboratory, 2002
 57. Etutu T G, Laohalidanond K, Kerdsuwan S. Gasification of municipal solid waste in a downdraft gasifier: analysis of tar formation. *Songklanakarin Journal of Science and Technology*, 2016, 38(2): 221–228
 58. Berrueco C, Montané D, Matas Güell B, del Alamo G. Effect of temperature and dolomite on tar formation during gasification of torrefied biomass in a pressurized fluidized bed. *Energy*, 2014, 66: 849–859
 59. Erkiaga A, Lopez G, Amutio M, Bilbao J, Olazar M. Influence of operating conditions on the steam gasification of biomass in a conical spouted bed reactor. *Chemical Engineering Journal*, 2014, 237: 259–267
 60. Qin Y H, Feng J, Li W Y. Formation of tar and its characterization during air-steam gasification of sawdust in a fluidized bed reactor. *Fuel*, 2010, 89(7): 1344–1347
 61. Klein A, Themelis N J. Energy recovery from municipal solid wastes by gasification. In: *11th North American Waste-to-Energy Conference*, Tampa: American Society of Mechanical Engineers, 2003, 241–252
 62. Shen Y, Yoshikawa K. Recent progresses in catalytic tar elimination during biomass gasification or pyrolysis—a review. *Renewable & Sustainable Energy Reviews*, 2013, 21: 371–392
 63. Di Carlo A, Borello D, Sisinni M, Savuto E, Venturini P, Bocci E, Kuramoto K. Reforming of tar contained in a raw fuel gas from biomass gasification using nickel-mayenite catalyst. *International Journal of Hydrogen Energy*, 2015, 40(30): 9088–9095
 64. Wolfesberger U, Aigner I, Hofbauer H. Tar content and composition in producer gas of fluidized bed gasification of

- wood-influence of temperature and pressure. *Environmental Progress & Sustainable Energy*, 2009, 28(3): 372–379
65. Nemanova V, Nordgreen T, Sjoström K. Green methane from biomass gasification: final report. Stockholm: KTH Royal Institute of Technology, 2010
66. Riis T, Hagen E F, Vie P J, Ulleberg Ø. Hydrogen production—gaps and priorities. IEA Hydrogen Implementing Agreement, 2006
67. Ghoneim S A, El-Salamony R A, El-Temtamy S A. Review on innovative catalytic reforming of natural gas to syngas. *World Journal of Engineering and Technology*, 2016, 4(01): 116–139
68. Obonukut M E, Alabi S B, Basse P G. Steam reforming of natural gas: a value addition to natural gas utilization in Nigeria. *Journal of Chemistry and Chemical Engineering*, 2016, 1: 28–41
69. Coll R, Salvado J, Farriol X, Montané D. Steam reforming model compounds of biomass gasification tars: conversion at different operating conditions and tendency towards coke formation. *Fuel Processing Technology*, 2001, 74(1): 19–31
70. Guan G, Kaewpanha M, Hao X, Abudula A. Catalytic steam reforming of biomass tar: prospects and challenges. *Renewable & Sustainable Energy Reviews*, 2016, 58: 450–461
71. Laosiripojana N, Sutthisripok W, Charojrochkul S, Assabumrungrat S. Development of Ni-Fe bimetallic based catalysts for biomass tar cracking/reforming: effects of catalyst support and Co-fed reactants on tar conversion characteristics. *Fuel Processing Technology*, 2014, 127: 26–32
72. Rached J A, El Hayek C, Dahdah E, Gennequion C, Aouad S, Tidahy H L, Estephane J, Nsouli B, Aboukaïs A, Abi-Aad E. Ni based catalysts promoted with cerium used in the steam reforming of toluene for hydrogen production. *International Journal of Hydrogen Energy*, 2016, 42: 12829–12840
73. Silveira E, Rabelo-Neto R, Noronha F. Steam reforming of toluene, methane and mixtures over Ni/ZrO₂ catalysts. *Catalysis Today*, 2017, 289: 289–301
74. Josuinkas F M, Quietete C P, Ribeiro N F, Souza M M V M. Steam reforming of model gasification tar compounds over nickel catalysts prepared from hydrotalcite precursors. *Fuel Processing Technology*, 2014, 121: 76–82
75. Ashok J, Kawi S. Steam reforming of toluene as a biomass tar model compound over CeO₂ promoted Ni/CaO-Al₂O₃ catalytic systems. *International Journal of Hydrogen Energy*, 2013, 38(32): 13938–13949
76. Chitsazan S, Sepehri S, Garbarino G, Carnasciali M M, Busca G. Steam reforming of biomass-derived organics: interactions of different mixture components on Ni/Al₂O₃ based catalysts. *Applied Catalysis B: Environmental*, 2016, 187: 386–398
77. Sehested J, Larsen N W, Falsig H, Hinnemann B. Sintering of nickel steam reforming catalysts: effective mass diffusion constant for Ni-OH at nickel surfaces. *Catalysis Today*, 2014, 228: 22–31
78. Sehested J. Four challenges for nickel steam-reforming catalysts. *Catalysis Today*, 2006, 111(1–2): 103–110
79. Vivanpatarakij S, Rulerk D, Assabumrungrat S. Removal of tar from biomass gasification process by steam reforming over nickel catalysts. *Chemical Engineering Transactions*, 2014, 37: 205–210
80. An L, Dong C, Yang Y, Zhang J, He L. The influence of Ni loading on coke formation in steam reforming of acetic acid. *Renewable Energy*, 2011, 36(3): 930–935
81. Wojcieszak R, Zieliński M, Monteverdi S, Bettahar M M. Study of nickel nanoparticles supported on activated carbon prepared by aqueous hydrazine reduction. *Journal of Colloid and Interface Science*, 2006, 299(1): 238–248
82. Park H J, Park S H, Sohn J M, Park J, Jeon J K, Kim S S, Park Y K. Steam reforming of biomass gasification tar using benzene as a model compound over various Ni supported metal oxide catalysts. *Bioresource Technology*, 2010, 101(1): S101–S103
83. Kim H W, Kang K M, Kwak H Y. Preparation of supported Ni catalysts with a core/shell structure and their catalytic tests of partial oxidation of methane. *International Journal of Hydrogen Energy*, 2009, 34(8): 3351–3359
84. Kaewpanha M, Kamjanakom S, Guan G, Hao X, Yang J, Abudula A. Removal of biomass tar by steam reforming over calcined scallop shell supported Cu catalysts. *Journal of Energy Chemistry*, 2017, 26(4): 660–666
85. Zhao X Y, Xue Y P, Yan C F, Wang Z, Guo C, Huang S. Sorbent assisted catalyst of Ni-CaO-La₂O₃ for sorption enhanced steam reforming of bio-oil with acetic acid as the model compound. *Chemical Engineering and Processing: Process Intensification*, 2017, 119: 106–112
86. Sisinni M, Di Carlo A, Bocci E, Micangeli A, Naso V. Hydrogen-rich gas production by sorption enhanced steam reforming of woodgas containing tar over a commercial Ni catalyst and calcined dolomite as CO₂ sorbent. *Energies*, 2013, 6(7): 3167–3181
87. Iida H, Noguchi K, Numa T, Igarashi A, Okumura K. Ru/12SrO–7Al₂O₃ (S1₂A₇) catalyst prepared by physical mixing with Ru (PPh₃)₃Cl₂ for steam reforming of toluene. *Catalysis Communications*, 2015, 72: 101–104
88. Reina T R, Ivanova S, Laguna O, Centeno M A, Odriozola J A. WGS and CO-PrO_x reactions using gold promoted copper-ceria catalysts: bulk CuO/CeO₂ vs. CuO/CeO₂/Al₂O₃ with low mixed oxide content. *Applied Catalysis B: Environmental*, 2016, 197: 62–72
89. Reina T R, Ivanova S, Delgado J J, Ivanov I. Viability of Au/CeO₂-ZnO/Al₂O₃ catalysts for pure hydrogen production by the water-gas shift reaction. *ChemCatChem*, 2014, 6(5): 1401–1409
90. Zhou H P, Wu H S, Shen J, Yin A X, Sun L D, Yan C H. Thermally stable Pt/CeO₂ hetero-nanocomposites with high catalytic activity. *Journal of the American Chemical Society*, 2010, 132(14): 4998–4999
91. Lin F H, Doong R A. Catalytic nanoreactors of Au@Fe₃O₄ yolk-shell nanostructures with various Au sizes for efficient nitroarene reduction. *Journal of Physical Chemistry C*, 2017, 121(14): 7844–7853
92. Nan Beurden P. On the catalytic aspects of steam-methane reforming. Report No.: I-04–003. Petten: Energy Research Centre of the Netherlands, 2004
93. Bossola F, Pereira-Hernández X I, Evangelisti C, Wang Y, Dal Santo V. Investigation of the promoting effect of Mn on a Pt/C catalyst for the steam and aqueous phase reforming of glycerol. *Journal of Catalysis*, 2017, 349: 75–83
94. Jeong J H, Lee J W, Seo D J, Seo Y, Yoon W L, Lee D K, Kim D H. Ru-doped Ni catalysts effective for the steam reforming of methane without the pre-reduction treatment with H₂. *Applied Catalysis A, General*, 2006, 302(2): 151–156

95. Xie C, Chen Y, Engelhard M H, Song C. Comparative study on the sulfur tolerance and carbon resistance of supported noble metal catalysts in steam reforming of liquid hydrocarbon fuel. *ACS Catalysis*, 2012, 2(6): 1127–1137
96. Zhou H, Zhang T, Sui Z, Zhu Y A, Han C, Zhu K, Zhou X. A single source method to generate Ru-Ni-MgO catalysts for methane dry reforming and the kinetic effect of Ru on carbon deposition and gasification. *Applied Catalysis B: Environmental*, 2018, 233: 143–159
97. Higo T, Saito H, Ogo S, Sugiura Y, Sekine Y. Promotive effect of Ba addition on the catalytic performance of Ni/LaAlO₃ catalysts for steam reforming of toluene. *Applied Catalysis A, General*, 2017, 530: 125–131
98. Oemar U, Ang M L, Hee W F, Hidajat K, Kawi S. Perovskite La_xM_{1-x}Ni_{0.8}Fe_{0.2}O₃ catalyst for steam reforming of toluene: crucial role of alkaline earth metal at low steam condition. *Applied Catalysis B: Environmental*, 2014, 148–149: 231–242
99. Kang S, Sub Kwak B, Kang M. Synthesis of ni-alkaline earth metals particles encapsulated by porous SiO₂ (NiMO@SiO₂) and their catalytic performances on ethanol steam reforming. *Ceramics International*, 2014, 40(9): 14197–14206
100. Yin K, Mahamulkar S, Xie J, Shibata H, Malek A, Li L, Jones C W, Agrawal P, Davis R J. Catalytic reactions of coke with dioxygen and steam over alkaline-earth-metal-doped cerium-zirconium mixed oxides. *Applied Catalysis A, General*, 2017, 535: 17–23
101. Yang L, Choi Y, Qin W, Chen H, Blinn K, Liu M, Liu P, Bai J, Tyson T A, Liu M. Promotion of water-mediated carbon removal by nanostructured barium oxide/nickel interfaces in solid oxide fuel cells. *Nature Communications*, 2011, 2(1): 357
102. Hu S, He L, Wang Y, Su S, Jiang L, Chen Q, Liu Q, Chi H, Xiang J, Sun L. Effects of oxygen species from Fe addition on promoting steam reforming of toluene over Fe-Ni/Al₂O₃ catalysts. *International Journal of Hydrogen Energy*, 2016, 41(40): 17967–17975
103. Karnjanakom S, Guan G, Asep B, Du X, Hao X, Samart C, Abudula A. Catalytic steam reforming of tar derived from steam gasification of sunflower stalk over ethylene glycol assisting prepared Ni/MCM-41. *Energy Conversion and Management*, 2015, 98: 359–368
104. Dam A H. Bimetallic catalyst system for steam reforming. Dissertation for the Doctorial Degree. Norway: Norwegian University of Science and Technology, 2015
105. Li D, Lu M, Aragaki K, Koike M, Nakagawa Y, Tomishige K. Characterization and catalytic performance of hydrotalcite-derived Ni-Cu alloy nanoparticles catalysts for steam reforming of 1-methylnaphthalene. *Applied Catalysis B: Environmental*, 2016, 192: 171–181
106. You X, Wang X, Ma Y, Liu J, Liu W, Xu X, Peng H, Li C, Zhou W, Yuan P, Chen X. Ni-Co/Al₂O₃ bimetallic catalysts for CH₄ steam reforming: elucidating the role of Co for improving coke resistance. *ChemCatChem*, 2014, 6(12): 3377–3386
107. Yoon Y, Kim H, Lee J. Enhanced catalytic behavior of Ni alloys in steam methane reforming. *Journal of Power Sources*, 2017, 359: 450–457
108. Ahmed T, Xiu S, Wang L, Shahbazi A. Investigation of Ni/Fe/Mg zeolite-supported catalysts in steam reforming of tar using simulated-toluene as model compound. *Fuel*, 2018, 211: 566–571
109. Koike M, Li D, Watanabe H, Nakagawa Y, Tomishige K. Comparative study on steam reforming of model aromatic compounds of biomass tar over Ni and Ni-Fe alloy nanoparticles. *Applied Catalysis A, General*, 2015, 506: 151–162
110. Li D, Koike M, Wang L, Nakagawa Y, Xu Y, Tomishige K. Regenerability of hydrotalcite-derived nickel-iron alloy nanoparticles for syngas production from biomass tar. *ChemSusChem*, 2014, 7(2): 510–522
111. Mukai D, Murai Y, Higo T, Ogo S, Sugiura Y, Sekine Y. Effect of Pt addition to Ni/La_{0.7}Sr_{0.3}AlO_{3-δ} catalyst on steam reforming of toluene for hydrogen production. *Applied Catalysis A, General*, 2014, 471: 157–164
112. Parizotto N, Zanchet D, Rocha K, Marques C M P, Bueno J M C. The effects of Pt promotion on the oxi-reduction properties of alumina supported nickel catalysts for oxidative steam-reforming of methane: temperature-resolved XAFS analysis. *Applied Catalysis A, General*, 2009, 366(1): 122–129
113. Moraes T S, Rabelo Neto R C, Ribeiro M C, Mattos L V, Kourtelesis M, Ladas S, Verykios X, Noronha F B. Ethanol conversion at low temperature over CeO₂-supported Ni-based catalysts. Effect of Pt addition to Ni catalyst. *Applied Catalysis B: Environmental*, 2016, 181: 754–768
114. Nurunnabi M, Fujimoto K I, Suzuki K, Li B, Kado S, Kunimori K, Tomishige K. Promoting effect of noble metals addition on activity and resistance to carbon deposition in oxidative steam reforming of methane over NiO-MgO solid solution. *Catalysis Communications*, 2006, 7(2): 73–78
115. Jaiswar V K, Katheria S, Deo G, Kunzru D. Effect of Pt doping on activity and stability of Ni/MgAl₂O₄ catalyst for steam reforming of methane at ambient and high pressure condition. *International Journal of Hydrogen Energy*, 2017, 42(30): 18968–18976
116. García-Diéguez M, Pieta I S, Herrera M C, Larrubia M A, Alemany L J. Nanostructured Pt- and Ni-based catalysts for CO₂-reforming of methane. *Journal of Catalysis*, 2010, 270(1): 136–145
117. Nabgan W, Tuan Abdullah T A, Mat R, Nabgan B, Gambo Y, Triwahyono S. Influence of Ni to Co ratio supported on ZrO₂ catalysts in phenol steam reforming for hydrogen production. *International Journal of Hydrogen Energy*, 2016, 41(48): 22922–22931
118. Luo N, Ouyang K, Cao F, Xiao T. Hydrogen generation from liquid reforming of glycerin over Ni-Co bimetallic catalyst. *Biomass and Bioenergy*, 2010, 34(4): 489–495
119. Zhang X, Yang C, Zhang Y, Xu Y, Shang S, Yin Y. Ni-Co catalyst derived from layered double hydroxides for dry reforming of methane. *International Journal of Hydrogen Energy*, 2015, 40(46): 16115–16126
120. Cao J P, Ren J, Zhao X Y, Wei X Y, Takarada T. Effect of atmosphere on carbon deposition of Ni/Al₂O₃ and Ni-loaded on lignite char during reforming of toluene as a biomass tar model compound. *Fuel*, 2018, 217: 515–521
121. Park S Y, Oh G, Kim K, Seo M W, Ra H W, Mun T Y, Lee J G, Yoon S J. Deactivation characteristics of Ni and Ru catalysts in tar steam reforming. *Renewable Energy*, 2017, 105: 76–83
122. Liu X, Yang X, Liu C, Chen P, Yue X, Zhang S. Low-temperature catalytic steam reforming of toluene over activated carbon supported nickel catalysts. *Journal of the Taiwan Institute of*

- Chemical Engineers, 2016, 65: 233–241
123. Valle B, Aramburu B, Remiro A, Bilbao J, Gayubo A G. Effect of calcination/reduction conditions of Ni/La₂O₃- α -Al₂O₃ catalyst on its activity and stability for hydrogen production by steam reforming of raw bio-oil/ethanol. *Applied Catalysis B: Environmental*, 2014, 147: 402–410
 124. Boukha Z, Jiménez-González C, de Rivas B, González-Velasco J R, Gutiérrez-Ortiz J I, López-Fonseca R. Synthesis, characterisation and performance evaluation of spinel-derived Ni/Al₂O₃ catalysts for various methane reforming reactions. *Applied Catalysis B: Environmental*, 2014, 158–159: 190–201
 125. Meng J, Wang X, Zhao Z, Wu X, Zheng A, Wei G, Huang Z, Li H. A highly carbon-resistant olivine thermally fused with metallic nickel catalyst for steam reforming of biomass tar model compound. *RSC Advances*, 2017, 7(62): 39160–39171
 126. Cárdenas-Espinosa D C, Vargas J C. Influence of the preparation conditions of Ca doped Ni/olivine catalysts on the improvement of gas quality produced by biomass gasification. *Studies in Surface Science and Catalysis*, 2010, 175: 385–388
 127. Courson C, Udron L, Świerczyński D, Kiennemann A. Hydrogen production from biomass gasification on nickel catalysts: tests for dry reforming of methane. *Catalysis Today*, 2002, 76(1): 75–86
 128. Cui D, Liu J, Yu J, Yue J, Su F, Xu G. Necessity of moderate metal-support interaction in Ni/Al₂O₃ for syngas methanation at high temperatures. *RSC Advances*, 2015, 5(14): 10187–10196
 129. Pandey D, Deo G. Effect of support on the catalytic activity of supported Ni-Fe catalysts for the CO₂ methanation reaction. *Journal of Industrial and Engineering Chemistry*, 2016, 33: 99–107
 130. Villoria J A, Mota N, Al-Sayari S, Alvarez-Galvan M C, Navarro R M, Luis Garcia Fierro J. Perovskites as catalysts in the reforming of hydrocarbons: a review. *Micro and Nanosystems*, 2012, 4(3): 231–252
 131. Lian J, Fang X, Liu W, Huang Q, Sun Q, Wang H, Wang X, Zhou W. Ni supported on LaFeO₃ perovskites for methane steam reforming: on the promotional effects of plasma treatment in H₂-Ar atmosphere. *Topics in Catalysis*, 2017, 60(12–14): 831–842
 132. Aman D, Radwan D, Ebaid M, Mikhail S, van Steen E. Comparing nickel and cobalt perovskites for steam reforming of glycerol. *Molecular Catalysis*, 2018, 452: 60–67
 133. Quitete C P, Manfro R L, Souza M M. Perovskite-based catalysts for tar removal by steam reforming: effect of the presence of hydrogen sulfide. *International Journal of Hydrogen Energy*, 2017, 42(15): 9873–9880
 134. Rapagná S, Provendier H, Petit C, Kiennemann A, Foscolo P U. Development of catalysts suitable for hydrogen or syn-gas production from biomass gasification. *Biomass and Bioenergy*, 2002, 22(5): 377–388
 135. Oemar U, Ang P S, Hidajat K, Kawi S. Promotional effect of Fe on perovskite LaNi_xFe_{1-x}O₃ catalyst for hydrogen production via steam reforming of toluene. *International Journal of Hydrogen Energy*, 2013, 38(14): 5525–5534
 136. Qi Y, Cheng Z, Zhou Z. Steam reforming of methane over ni catalysts prepared from hydrotalcite-type precursors: catalytic activity and reaction kinetics. *Chinese Journal of Chemical Engineering*, 2015, 23(1): 76–85
 137. Noor T. Sorption enhanced high temperature water gas shift reaction: materials and catalysis. Dissertation for the Doctoral Degree. Trondheim: Norwegian University of Science and Technology, 2013
 138. Mitran G, Mieritz D G, Seo D K. Hydrotalcites with vanadium, effective catalysts for steam reforming of toluene. *International Journal of Hydrogen Energy*, 2017, 42(34): 21732–21740
 139. Nguyen-Thanh D, Duarte de Farias A M, Fraga M A. Characterization and activity of vanadia-promoted Pt/ZrO₂ catalysts for the water-gas shift reaction. *Catalysis Today*, 2008, 138(3–4): 235–238
 140. Ballarini N, Battisti A, Cavani F, Cericola A, Lucarelli C, Racioppi S, Arpentinier P. The oxygen-assisted transformation of propane to CO_x/H₂ through combined oxidation and wgs reactions catalyzed by vanadium oxide-based catalysts. *Catalysis Today*, 2006, 116(3): 313–323
 141. Kokumai T M, Cantane D A, Melo G T, Paulucci L B, Zanchet D. VO_x-Pt/Al₂O₃ catalysts for hydrogen production. *Catalysis Today*, 2017, 289: 249–257
 142. Labhasetwar N, Saravanan G, Kumar Megarajan S, Manwar N, Khobragade R, Doggali P, Grasset F. Perovskite-type catalytic materials for environmental applications. *Science and Technology of Advanced Materials*, 2015, 16(3): 036002
 143. Yousaf B. Hydrotalcite based ni-co bi-metallic catalysts for steam reforming of methane. NTNU, 2016
 144. Higo T, Hashimoto T, Mukai D, Nagatake S, Ogo S, Sugiura Y, Sekine Y. Effect of hydrocarbon structure on steam reforming over Ni/perovskite catalyst. *Journal of the Japan Petroleum Institute*, 2015, 58(2): 86–96
 145. Zarei Senseni A, Seyed Fattahi S M, Rezaei M, Meshkani F. A comparative study of experimental investigation and response surface optimization of steam reforming of glycerol over nickel nano-catalysts. *International Journal of Hydrogen Energy*, 2016, 41(24): 10178–10192
 146. Gil M V, Feroso J, Rubiera F, Chen D. H₂ production by sorption enhanced steam reforming of biomass-derived bio-oil in a fluidized bed reactor: an assessment of the effect of operation variables using response surface methodology. *Catalysis Today*, 2015, 242: 19–34
 147. Huang C, Xu C, Wang B, Hu X, Li J, Liu J, Liu J, Li C. High production of syngas from catalytic steam reforming of biomass glycerol in the presence of methane. *Biomass and Bioenergy*, 2018, 119: 173–178
 148. Zhang C, Hu X, Yu Z, Zhang Z, Chen G, Li C, Liu Q, Xiang J, Wang Y, Hu S. Steam reforming of acetic acid for hydrogen production over attapulgite and alumina supported Ni catalysts: impacts of properties of supports on catalytic behaviors. *International Journal of Hydrogen Energy*, 2019, 44(11): 5230–5244
 149. Jess A. Catalytic upgrading of tarry fuel gases: a kinetic study with model components. *Chemical Engineering and Processing: Process Intensification*, 1996, 35(6): 487–494
 150. Quitete C P, Souza M M. Application of brazilian dolomites and mixed oxides as catalysts in tar removal system. *Applied Catalysis A, General*, 2017, 536: 1–8
 151. Pant K K, Jain R, Jain S. Renewable hydrogen production by steam reforming of glycerol over Ni/CeO₂ catalyst prepared by precipitation deposition method. *Korean Journal of Chemical Engineering*, 2011, 28(9): 1859–1866

152. Kimura T, Miyazawa T, Nishikawa J, Kado S, Okumura K, Miyao T, Naito S, Kunimori K, Tomishige K. Development of Ni catalysts for tar removal by steam gasification of biomass. *Applied Catalysis B: Environmental*, 2006, 68(3–4): 160–170
153. Jeon J, Nam S, Ko C H. Rapid evaluation of coke resistance in catalysts for methane reforming using low steam-to-carbon ratio. *Catalysis Today*, 2018, 309: 140–146
154. Li Q, Wang Q, Kayamori A, Zhang J. Experimental study and modeling of heavy tar steam reforming. *Fuel Processing Technology*, 2018, 178: 180–188
155. Tao J, Zhao L, Dong C, Lu Q, Du X, Dahlquist E. Catalytic steam reforming of toluene as a model compound of biomass gasification tar using Ni-CeO₂/SBA-15 catalysts. *Energies*, 2013, 6(7): 3284–3296
156. Gao N, Wang X, Li A, Wu C, Yin Z. Hydrogen production from catalytic steam reforming of benzene as tar model compound of biomass gasification. *Fuel Processing Technology*, 2016, 148: 380–387
157. Gao N, Liu S, Han Y, Xing C, Li A. Steam reforming of biomass tar for hydrogen production over NiO/ceramic foam catalyst. *International Journal of Hydrogen Energy*, 2015, 40(25): 7983–7990
158. Zhang R, Wang H, Hou X. Catalytic reforming of toluene as tar model compound: effect of Ce and Ce-Mg promoter using Ni/olivine catalyst. *Chemosphere*, 2014, 97: 40–46
159. Liang T, Wang Y, Chen M, Yang Z, Liu S, Zhou Z, Li X. Steam reforming of phenol-ethanol to produce hydrogen over bimetallic NiCu catalysts supported on sepiolite. *International Journal of Hydrogen Energy*, 2017, 42(47): 28233–28246
160. Italiano C, Luchters N T J, Pino L, Fletcher J V, Specchia S, Fletcher J C Q, Vita A. High specific surface area supports for highly active Rh catalysts: syngas production from methane at high space velocity. *International Journal of Hydrogen Energy*, 2018, 43(26): 11755–11765
161. Compagnoni M, Tripodi A, Rossetti I. Parametric study and kinetic testing for ethanol steam reforming. *Applied Catalysis B: Environmental*, 2017, 203: 899–909
162. Pashchenko D. Numerical study of steam methane reforming over a pre-heated Ni-based catalyst with detailed fluid dynamics. *Fuel*, 2019, 236: 686–694
163. Kim S, Chun D, Rhim Y, Lim J, Kim S, Choi H, Lee S, Yoo J. Catalytic reforming of toluene using a nickel ion-exchanged coal catalyst. *International Journal of Hydrogen Energy*, 2015, 40(35): 11855–11862
164. Chen G, Tao J, Liu C, Yan B, Li W, Li X. Hydrogen production via acetic acid steam reforming: a critical review on catalysts. *Renewable & Sustainable Energy Reviews*, 2017, 79: 1091–1098
165. Lange J P. Catalysis for biorefineries-performance criteria for industrial operation. *Catalysis Science & Technology*, 2016, 6(13): 4759–4767
166. Hashemnejad S M, Parvari M. Deactivation and regeneration of nickel-based catalysts for steam-methane reforming. *Chinese Journal of Catalysis*, 2011, 32(1–2): 273–279
167. Argyle M, Bartholomew C. Heterogeneous catalyst deactivation and regeneration: a review. *Catalysts*, 2015, 5(1): 145–269
168. Trimm D L. Catalysts for the control of coking during steam reforming. *Catalysis Today*, 1999, 49(1–3): 3–10
169. Kathiraser Y, Ashok J, Kawi S. Synthesis and evaluation of highly dispersed SBA-15 supported Ni-Fe bimetallic catalysts for steam reforming of biomass derived tar reaction. *Catalysis Science & Technology*, 2016, 6(12): 4327–4336
170. Iida H, Fujiyama A, Igarashi A, Okumura K. Steam reforming of toluene over Ru/SrCo₃-Al₂O₃ catalysts. *Fuel Processing Technology*, 2017, 168: 50–57
171. Oemar U, Ang M L, Hidajat K, Kawi S. Enhancing performance of Ni/La₂O₃ catalyst by Sr-modification for steam reforming of toluene as model compound of biomass tar. *RSC Advances*, 2015, 5(23): 17834–17842
172. Broda M, Kierzkowska A M, Müller C R. Sorbent-enhanced steam methane reforming reaction studied over a Ca-based CO₂ sorbent and Ni catalyst. *Chemical Engineering & Technology*, 2013, 36(9): 1496–1502
173. Quitete C P, Bittencourt R C P, Souza M M. Steam reforming of tar using toluene as a model compound with nickel catalysts supported on hexaaluminates. *Applied Catalysis A, General*, 2014, 478: 234–240
174. Dou X, Veksha A, Chan W P, Oh W D, Liang Y N, Teoh F, Mohamed D K B, Giannis A, Lisak G, Lim T T. Poisoning effect of H₂S and HCl on the naphthalene steam reforming and water-gas shift activities of Ni and Fe catalysts. *Fuel*, 2019, 241: 1008–1018
175. Ashok J, Das S, Dewangan N, Kawi S. H₂S and NO_x tolerance capability of CeO₂ doped La_{1-x}Ce_{2x}Co_{0.5}Ti_{0.5}O_{3-δ} perovskites for steam reforming of biomass tar model reaction. *Energy Conversion and Management: X*, 2019, 1: 100003
176. Veksha A, Giannis A, Oh W D, Chang V W C, Lisak G, Lim T T. Catalytic activities and resistance to HCl poisoning of Ni-based catalysts during steam reforming of naphthalene. *Applied Catalysis A, General*, 2018, 557: 25–38
177. Xu C C, Donald J, Byambajav E, Ohtsuka Y. Recent advances in catalysts for hot-gas removal of tar and NH₃ from biomass gasification. *Fuel*, 2010, 89(8): 1784–1795
178. Stemmler M, Müller M. Chemical hot gas cleaning concept for the “chrisgas” process. *Biomass and Bioenergy*, 2011, 35: S105–S115
179. Torres W, Pansare S S, Goodwin J G Jr. Hot gas removal of tars, ammonia, and hydrogen sulfide from biomass gasification gas. *Catalysis Reviews*, 2007, 49(4): 407–456
180. Garbarino G, Lagazzo A, Riani P, Busca G. Steam reforming of ethanol-phenol mixture on Ni/Al₂O₃: effect of Ni loading and sulphur deactivation. *Applied Catalysis B: Environmental*, 2013, 129: 460–472
181. Zuber C, Hochenauer C, Kienberger T. Test of a hydrodesulfurization catalyst in a biomass tar removal process with catalytic steam reforming. *Applied Catalysis B: Environmental*, 2014, 156–157: 62–71
182. Li C, Hirabayashi D, Suzuki K. A crucial role of O²⁻ and O²²⁻ on mayenite structure for biomass tar steam reforming over Ni/Ca₁₂Al₁₄O₃₃. *Applied Catalysis B: Environmental*, 2009, 88(3–4): 351–360
183. Savuto E, Navarro R, Mota N, Di Carlo A, Bocci E, Carlini M, Fierro J L G. Steam reforming of tar model compounds over Ni/mayenite catalysts: effect of Ce addition. *Fuel*, 2018, 224: 676–686

184. Mawdsley J R, Krause T R. Rare earth-first-row transition metal perovskites as catalysts for the autothermal reforming of hydrocarbon fuels to generate hydrogen. *Applied Catalysis A, General*, 2008, 334(1–2): 311–320
185. Hepola J, Simell P. Sulphur poisoning of nickel-based hot gas cleaning catalysts in synthetic gasification gas: I. Effect of different process parameters. *Applied Catalysis B: Environmental*, 1997, 14(3–4): 287–303
186. Avasthi K S, Reddy R N, Patel S. Challenges in the production of hydrogen from glycerol—a biodiesel byproduct via steam reforming process. *Procedia Engineering*, 2013, 51: 423–429
187. Schwengber C A, Alves H J, Schaffner R A, da Silva F A, Sequinel R, Bach V R, Ferracin R J. Overview of glycerol reforming for hydrogen production. *Renewable & Sustainable Energy Reviews*, 2016, 58: 259–266
188. Chapin D, Kiffer S, Nestell J. The very high temperature reactor: a technical summary. Alexandria, VA: MPR Associates Inc., 2004
189. Compagne P A. Multi-tubular steam reformer and process for catalytic steam reforming of a hydrocarbonaceous feedstock. 2014, US Patent Application: 14/008,906
190. Patra A. Oxide dispersion strengthened high temperature alloys. *Journal of Materials Science and Nanomaterials*, 2017, 1(1): e101
191. Karim A, Bravo J, Gorm D, Conant T, Datye A. Comparison of wall-coated and packed-bed reactors for steam reforming of methanol. *Catalysis Today*, 2005, 110(1–2): 86–91
192. Kundu A, Park J, Ahn J, Park S S, Shul Y G, Han H S. Micro-channel reactor for steam reforming of methanol. *Fuel*, 2007, 86(9): 1331–1336
193. Iulianelli A, Ribeiro P, Mendes A, Basile A. Methanol steam reforming for hydrogen generation via conventional and membrane reactors: a review. *Renewable & Sustainable Energy Reviews*, 2014, 29: 355–368
194. Alauddin Z A B Z, Lahijani P, Mohammadi M, Mohamed A R. Gasification of lignocellulosic biomass in fluidized beds for renewable energy development: a review. *Renewable & Sustainable Energy Reviews*, 2010, 14(9): 2852–2862
195. Nam H, Wang Z, Shanmugam S R, Adhikari S, Abdoulmoumine N. Chemical looping dry reforming of benzene as a gasification tar model compound with Ni- and Fe-based oxygen carriers in a fluidized bed reactor. *International Journal of Hydrogen Energy*, 2018, 43(41): 18790–18800
196. Bassano C, Deiana P. Carbon dioxide reforming of tar during biomass gasification. *Chemical Engineering Transactions*, 2014, 37: 97–102
197. Abou Rached J, Cesario M R, Estephane J, Tidahy H L, Gennequin C, Aouad S, Aboukais A, Abi-Aad E. Effects of cerium and lanthanum on Ni-based catalysts for CO₂ reforming of toluene. *Journal of Environmental Chemical Engineering*, 2018, 6(4): 4743–4754
198. Bao X, Kong M, Lu W, Fei J, Zheng X. Performance of Co/MgO catalyst for CO₂ reforming of toluene as a model compound of tar derived from biomass gasification. *Journal of Energy Chemistry*, 2014, 23(6): 795–800
199. Jang W J, Shim J O, Kim H M, Yoo S Y, Roh H S. A review on dry reforming of methane in aspect of catalytic properties. *Catalysis Today*, 2019, 34: 15–26
200. Rostrupnielsen J, Hansen J B. CO₂-reforming of methane over transition metals. *Journal of Catalysis*, 1993, 144(1): 38–49
201. Yu X, Wang N, Chu W, Liu M. Carbon dioxide reforming of methane for syngas production over La-promoted NiMgAl catalysts derived from hydrotalcites. *Chemical Engineering Journal*, 2012, 209: 623–632
202. Wang Z, Oemar U, Ang M L, Kawi S. Oxidative steam reforming of biomass tar model compound via catalytic BaBi_{0.05}Co_{0.8}Nb_{0.15}O_{3-δ} hollow fiber membrane reactor. *Journal of Membrane Science*, 2016, 510: 417–425
203. Mendiara T, Johansen J M, Utrilla R, Geraldo P, Jensen A D, Glarborg P. Evaluation of different oxygen carriers for biomass tar reforming (I): carbon deposition in experiments with toluene. *Fuel*, 2011, 90(3): 1049–1060
204. Sengodan S, Lan R, Humphreys J, Du D, Xu W, Wang H, Tao S. Advances in reforming and partial oxidation of hydrocarbons for hydrogen production and fuel cell applications. *Renewable & Sustainable Energy Reviews*, 2018, 82: 761–780
205. Kolb G. Fuel processing: for fuel cells. *Platinum Metals Review*, 2008, 53(3): 172–173
206. Lin Y C. Catalytic valorization of glycerol to hydrogen and syngas. *International Journal of Hydrogen Energy*, 2013, 38(6): 2678–2700
207. Nabgan W, Tuan Abdullah T A, Mat R, Nabgan B, Gambo Y, Ibrahim M, Ahmad A, Jalil A A, Triwahyono S, Saeh I. Renewable hydrogen production from bio-oil derivative via catalytic steam reforming: an overview. *Renewable & Sustainable Energy Reviews*, 2017, 79: 347–357
208. Di Giuliano A, Gallucci K. Sorption enhanced steam methane reforming based on nickel and calcium looping: a review. *Chemical Engineering and Processing—Process Intensification*, 2018, 130: 240–252
209. Xie H, Yu Q, Lu H, Zhang Y, Zhang J, Qin Q. Thermodynamic study for hydrogen production from bio-oil via sorption-enhanced steam reforming: comparison with conventional steam reforming. *International Journal of Hydrogen Energy*, 2017, 42(48): 28718–28731
210. Di Giuliano A, Giancaterino F, Courson C, Foscolo P U, Gallucci K. Development of a Ni-CaO-mayenite combined sorbent-catalyst material for multicycle sorption enhanced steam methane reforming. *Fuel*, 2018, 234: 687–699
211. Wassie S A, Medrano J A, Zaabout A, Cloete S, Melendez J, Tanaka D A P, Amini S, van Sint Annaland M, Gallucci F. Hydrogen production with integrated CO₂ capture in a membrane assisted gas switching reforming reactor: proof-of-concept. *International Journal of Hydrogen Energy*, 2018, 43(12): 6177–6190
212. Dou B, Wang C, Song Y, Chen H, Jiang B, Yang M, Xu Y. Solid sorbents for *in-situ* CO₂ removal during sorption-enhanced steam reforming process: a review. *Renewable & Sustainable Energy Reviews*, 2016, 53: 536–546
213. Zhang L, Hu X, Hu K, Hu C, Zhang Z, Liu Q, Hu S, Xiang J, Wang Y, Zhang S. Progress in the reforming of bio-oil derived carboxylic acids for hydrogen generation. *Journal of Power Sources*, 2018, 403: 137–156
214. Liu Y, Goeltl F, Ro I, Ball M R, Sener C, Aragão I B, Zanchet D,

- Huber G W, Mavrikakis M, Dumesic J A. Synthesis gas conversion over Rh-based catalysts promoted by Fe and Mn. *ACS Catalysis*, 2017, 7(7): 4550–4563
215. Sharma Y C, Kumar A, Prasad R, Upadhyay S N. Ethanol steam reforming for hydrogen production: latest and effective catalyst modification strategies to minimize carbonaceous deactivation. *Renewable & Sustainable Energy Reviews*, 2017, 74: 89–103
216. Sinaei Nobandegani M, Sardashti Birjandi M R, Darbandi T, Khalilipour M M, Shahraki F, Mohebbi-Kalhari D. An industrial steam methane reformer optimization using response surface methodology. *Journal of Natural Gas Science and Engineering*, 2016, 36: 540–549
217. Lior N. Quantifying sustainability for energy development. *Energy Bull*, 2015, 19: 8–24